defined their disease as ARVC (Figure 4).

Parameters between the CHF and VT groups are compared in Table II. Mean age at onset in the CHF group was significantly higher than that in the VT group (66.0 ± 4.0 versus 44.5 ± 14.8 years, $P = 0.02$). The CHF group showed significantly higher mortality compared to the VT group ($P < 0.001$) (Figure 5). There were no significant differences according to sex, ECG abnormality (complete or incomplete right bundle-branch block, Epsilon-wave, T-wave inversion in the right precordial leads in the absence of right bundle-branch block), and RV dilatation between the two groups at initial evaluation.

## Discussion

In this study, we found that ARVC patients with CHF onset had a poor prognosis, and recurrence of VT was greater than 50% in patients treated with RFCA treatment. This recurrence rate was not less than that in patients without RFCA treatment. ICD therapy did not improve mortality in comparison with RFCA or medical treatment but did significantly reduce rehospitalization compared with RFCA therapy.

One of the main purposes of therapy for ARVC patients is prevention of SCD because ARVC is a major cause of ventricular arrhythmias and sudden death in young people and athletes. ICD therapy is increasingly used for secondary and also primary prevention of sudden death in patients with ARVC and improves their long-term prognosis and survival.[5,6] Another report found that patients with ARVC treated with an ICD have an excellent prognosis,[12] and Hodgkinson, *et al* reported that the 5-year mortality rate of male ARVC patients with ICD therapy was 0% compared to 28% in control patients.[13]

Mild hypokinesis of left ventricular wall motion has been reported at onset of ARVC, but CHF as a manifestation of ARVC is rare.[1,14] However, a case of late-onset ARVC manifesting with CHF at age > 60 has been reported.[15] Other investigators reported an increase in left ventricular end-diastolic volume with normal ejection fraction in adult patients with ARVC in comparison to young patients with the disease.[16] Basso, *et al* reported the prognosis of 30 patients with ARVC: 24 died from SCD and 3 from CHF, and 3 patients underwent cardiac transplantation due to CHF. They also indicated that the mean age of CHF manifestation was older than that in other patients without CHF.[17] Hulot, *et al* reported that progressive heart failure as a cause of death in ARVC patients was twice as frequent as SCD.[10] In the present study, 4 patients died of CHF and one died of ventricular arrhythmia. Age at the time of death in all 4 patients who died of CHF was > 60 years (average age, 67.8 ± 6.6 years). Roguin also reported on a patient with ARVC who had end-stage disease with severe biventricular dysfunction and cavity dilation after ICD implantation and who subsequently underwent heart transplantation.[18] One of our patients also died of progressive heart failure 32 months after ICD implantation without VT recurrence. The diagnosis was established in all CHF group patients at autopsy. The existence of fibro-fatty replacement in both ventricles revealed that CHF progressed from right ventricular failure to biventricular failure leading to death by progressive heart failure.

From these data we conclude that prevention of SCD with ICD therapy improves survival rates of patients with early- to mid-stage ARVC, but CHF becomes the main clinical problem in the final stage of ARVC. Some of our patients also showed insidious progression of right ventricular disease without manifesting electrical disturbances leading to left ventricular involvement. In these cases, left ventricular failure can be the initial clinical symptom. The treatment of heart failure was difficult in all of these patients, and they died rapidly of progressive CHF. Elderly ARVC patients presenting with CHF clearly have a very poor prognosis.

The published results of catheter ablation in ARVC show that acute success can be achieved in 60-90% of patients. However, during long-term follow-up of 3-5 years, recurrence rates of as high as 50-70% were reported.[5,6] The pros and cons of the efficacy of RFCA with electroanatomic mapping to suppress VT were also reported.[19-21] We used electroanatomic mapping techniques in one patient to suppress frequent VT recurrence after RFCA and ICD therapies. We consider the efficacy of the electroanatomic mapping technique to be controversial. In the present report, we obtained a 68.4% acute success rate with RFCA, whereas the VT recurrence rate was 52.6% during the observation period. These results indicate that RFCA may be effective to suppress VT occurrence, but it may not effectively prevent VT recurrence over the long term.

Although there has been no prospective randomized trial comparing ICD implantation with RFCA in patients with ARVC, ICD implantation is considered the most appropriate therapeutic option to prevent life-threatening VT recurrences and sudden death.[6,7] It was reported that 66% of the ARVC patients undergoing ICD implantation for prevention of VT had at least one appropriate intervention during a 4.4 ± 2.9-year follow-up period.[22] We found that RFCA treatment was comparable to that of ICD implantation to prevent cardiovascular death. However, ICD treatment statistically reduced the frequency of hospitalization in comparison to that with RFCA. We speculate that patients with recurrent VT after RFCA are more likely to be hospitalized in Japan than are patients with VT terminated by ICD. We also speculate that Japanese cardiologists tend to perform RFCA to prevent VT in ARVC patients because appropriate clinical data on the long-term effect of RFCA therapy for ARVC are not yet available. The results of the present study suggest that the effects of ICD implantation in improving the ARVC patient's quality of life are superior to those of RFCA, at least in regard to rehospitalization.

**Study limitations:** This study has some limitations. First, it was a retrospective and not a case controlled study. Second, our data did not include ARVC patients manifesting with sudden cardiac death. Third, the majority of the study population admitted to our hospitals for treatment of ventricular arrhythmias included several patients introduced from other hospitals due to recurrence of VT after RFCA therapy. Thus, there may be patient selection bias, and the patients in this study may not adequately represent the general ARVC population in Japan. Fourth, the number of patients is relatively small, and only two patients died of ARVC in the VT group. Fifth, the observation period may have been

too short to adequately address the natural clinical course of this disease. Furthermore, because remarkable progress has been made recently in the pharmacologic prevention of ventricular arrhythmia, the effects of these new agents should have been evaluated.

**Conclusion:** In the present study, a minor but significant population of patients presented with CHF as their initial manifestation of ARVC. The prognosis of these patients may be very poor. Recurrence of VT was relatively higher in the patients treated with RFCA therapy, and this rate was not reduced by additional RFCA therapy. ICD therapy did not improve the mortality rate in comparison with RFCA in our patients, but it did significantly reduce the number of hospitalizations in comparison with RFCA therapy.

## References


1. Marcus FI, Fontaine GH, Guiraudon G, *et al.* Right ventricular dysplasia: a report of 24 adult cases. Circulation 1982; 65: 384-98.
2. Thiene G, Nava A, Corrado D, Rossi L, Pennelli N. Right ventricular cardiomyopathy and sudden death in young people. N Engl J Med 1988; 318: 129-33.
3. Wichter T, Borrggrefe M, Haverkamp W, Chen X, Breithardt G. Efficacy of antiarrhythmic drugs in patients with arrhythmogenic right ventricular disease. Results in patients with inducible and noninducible ventricular tachycardia. Circulation 1992; 86: 29-37.
4. Klein H, Frank G, Werner PC, Borst HG, Lichtlen PR. Surgical possibilities in the treatment of ventricular tachycardia. Herz 1984; 9: 90-101. (German)
5. Corrado D, Basso C, Thiene G. Arrhythmogenic right ventricular cardiomyopathy: diagnosis, prognosis, and treatment. Heart 2000; 83: 588-95. (Review)
6. Wichter T, Paul TM, Eckardt L, *et al.* Arrhythmogenic right ventricular cardiomyopathy. Antiarrhythmic drugs, catheter ablation, or ICD. Herz 2005; 30: 91-101. (Review)
7. Boriani G, Artale P, Biffi M, *et al.* Outcome of cardioverter-defibrillator implant in patients with arrhythmogenic right ventricular cardiomyopathy. Heart Vessels 2007; 22: 184-92.
8. Corrado D, Leoni L, Link MS, *et al.* Implantable Cardioverter-defibrillator therapy for prevention of sudden death in patients with arrhythmogenic right ventricular cardiomyopathy/dysplasia. Circulation 2003; 108: 3048-91.
9. Tomé Esteban MT, García-Pinilla JM, McKenna WJ. Update in arrhythmogenic right ventricular cardiomyopathy: genetic, clinical presentation and risk statification. Rev Esp Cardiol 2004; 57: 757-67. (Review) (Spanish)
10. Hulot JS, Jouven X, Empana JP, Frank R, Fontaine G. Natural history and risk stratification of arrhythmogenic right ventricular dysplasia/cardiomyopathy. Circulation 2004; 110: 1879-84. (Review)
11. McKenna WJ, Thiene G, Nava A, *et al.* Diagnosis of arrhythmogenic right ventricular dysplasia/cardiomyopathy. Task Force of the Working Group Myocardial and Pericardial Disease of the European Society of Cardiology and of the Scientific Council on Cardiomyopathies of the International Society and Federation of Cardiology. Br Heart J 1994; 71: 215-8.
12. Dalal D, Nasir K, Bomma C, *et al.* Arrhythmogenic right ventricular dysplasia: a United States experience. Circulation 2005; 112: 3823-32.
13. Hodgkinson KA, Parfrey PS, Bassett AS, *et al.* The impact of implantable cardioverter-difibrillator therapy on survival in autosomal-dominant arrhythmogenic right ventricular cardiomyopathy (ARVD5). J Am Coll Cardiol 2005; 45: 400-8.
14. Cho Y, Park T, Shin D, *et al.* Clinical manifestations of arrhythmogenic right ventricular cardiomyopathy in Korean patients. Int J Cardiol 2007; 122: 137-42.
15. Frigo G, Bauce B, Basso C, Nava A. Late-onset arrhythmogenic right ventricular cardiomyopathy. J Cardiovasc Med (Hagerstown) 2006; 7: 74-6.
16. Daliento L, Turrini P, Nava A, *et al.* Arrhythmogenic ventricular cardiomyopathy in young versus adult patients: similarities and differences. J Am Coll Cardiol 1995; 25: 655-64.
17. Basso C, Thiene G, Corrado D, Angelini A, Nava A, Valente M. Arrhythmogenic right ventricular cardiomyopathy. Dysplasia, dystrophy, or myocarditis? Circulation 1996; 94: 983-91.
18. Roguin A, Bomma CS, Nasir K, *et al.* Implantable cardioverter-defibrillators in patients with arrhythmogenic right ventricular dysplasia/cardiomyopathy. J Am Coll Cardiol 2004; 43: 1843-52.
19. Marchlinski FE, Zado E, Dixit S, *et al.* Electroanatomic substrate and outcome of catheter ablative therapy for ventricular tachycardia in setting of right ventricular cardiomyopathy. Circulation 2004; 110: 2293-8.
20. Satomi K, Kurita T, Suyama K, *et al.* Catheter ablation of stable and unstable ventricular tachycardia in patients with arrhythmogenic right ventricular dysplasia. J Cardiovasc Electrophysiol 2006; 17: 469-76.
21. Dalal D, Jain R, Tandri H, *et al.* Long-term efficacy of catheter ablation of ventricular tachycardia in patients with arrhythmogenic right ventricular dysplasia/cardiomyopathy. J Am Coll Cardiol 2007; 50: 432-40.
22. Piccini JP, Dalal D, Roguin A, *et al.* Predictor of appropriate implantable defibrillator therapies in patients with arrhythmogenic right ventricular dysplasia. Heart Rhythm 2005; 2: 1188-94.

# Granular Swollen Epithelial Cells: A Histologic and Diagnostic Marker for Mitochondrial Nephropathy

*Akimitsu Kobayashi, MD,* Yu-ichi Goto, MD, PhD,† Michio Nagata, MD, PhD,‡ and Yutaka Yamaguchi, MD§*

**Abstract:** Focal segmental glomerulosclerosis (FSGS) is a progressive kidney disease, and mitochondrial disease known to be a primary malady for secondary FSGS. Mitochondrial nephropathy with FSGS is diagnosed by genetic analysis or electron microscopy when it is suspected. As adequate morphologic features to diagnose mitochondrial nephropathy by light microscopy are lacking, this study used 10 cases with genetically proven mitochondrial disease and analyzed the kidney samples obtained by biopsy (n = 7) or autopsy (n = 3). We found granular swollen epithelial cells (GSECs) among the distal tubuli and collecting ducts in all patients, whereas such features were absent in IgA nephropathy, primary FSGS, and interstitial nephritis. Ultrastructural analysis of GSECs displayed accumulation of abnormal-shaped mitochondria in GSECs. To test whether GSECs were really associated with mitochondrial mutations, laser-captured single GSECs in 1 case with a position where 3,271 mutation were measured using a single-cell PCR analysis. This revealed that the mutant load of GSECs was significantly higher than normal-appearing epithelial cells within the same sample (63.4 ± 17.8% vs. 32.5 ± 4.6%; $P < 0.0001$). This is direct evidence that GSEC is a characteristic cellular feature, indicating cells with mutant mitochondrial DNA accumulation. In addition, the incidence of GSECs did not correlate with serum creatinine levels, proteinuria, percent glomerulosclerosis, tubulointerstitial changes, or arteriolar hyalinosis, suggesting that GSECs per se may not cause tissue damage. In conclusion, GSEC is a distinct morphologic feature suggesting mitochondrial nephropathy and is a useful tool to identify secondary FSGS on the basis of mitochondrial abnormalities.

From the *Division of Kidney and Hypertension, Department of Internal Medicine, The Jikei University School of Medicine; †Department of Mental Retardation and Birth Defect Research, National Institute of Neuroscience, National Center of Neurology and Psychiatry, Tokyo; ‡Department of Pathology, Graduate School of Comprehensive Human Sciences, University of Tsukuba, Tsukuba, Ibaraki; and §Department of Pathology, Kashiwa Hospital, The Jikei University School of Medicine, Chiba, Japan.

This work was supported in part by a Research Grant (18A-5) for Nervous and Mental Disorders from the Ministry of Health, Labour and Welfare of Japan (Y.G.) and a grant of the Comprehensive Research Project on Health Sciences Focusing on Drug Innovation (KHD2207) from the Japan Health Sciences Foundation (Y.G.).

The authors report no conflict of interest.

Correspondence: Akimitsu Kobayashi, MD, Division of Kidney and Hypertension, Department of Internal Medicine, The Jikei University School of Medicine, 3-25-8, Nishi-shinbashi, Minato-ku, Tokyo 105-8471, Japan (e-mail: akimitsu@kk.iij4u.or.jp).



**Key Words:** mitochondrial nephropathy, focal segmental glomerulosclerosis, mitochondrial disease

(*Am J Surg Pathol* 2010;34:262–270)

Focal segmental glomerulosclerosis (FSGS), a progressive kidney disease often leading to chronic renal failure, consists of heterogeneous disorders, including idiopathic or secondary forms. The majority of FSGS exists as a secondary form associated with various systemic diseases, including remnant kidney, vesicoureteral reflux, obesity, and virus-associated, genetic, drug-induced, and cyanotic heart disease.[1,3,13,15] Determination of secondary FSGS is important because the therapeutic strategy is different depending on the primary disease. Among several diseases accompanying secondary FSGS, mitochondrial disease is unique for its clinical features and the mechanism of FSGS occurrence.[6,10,12,14]

Mitochondrial diseases are multisystemic disorders that primarily involve skeletal muscle, the central nervous system, and cardiac muscle.[4,7] The diseases also complicate kidney disease of various features, including FSGS, Fanconi syndrome, and Bartter syndrome.[2,6,8,10,12,14,20,21] The diagnosis of mitochondrial diseases is usually made with blood samples, but is often difficult because the proportion of mutant mitochondrial DNA (mtDNA) varies in different cell types. Furthermore, mitochondrial abnormalities basically occur in a cell-specific manner, and thus, abnormalities in a blood sample do not necessarily fully explain that a mitochondrial abnormality is the cause of organ damage. In this context, direct examination of mitochondrial abnormalities in damaged tissue in situ is more convincing for a diagnosis. Site-specific mitochondrial abnormalities have been established by myopathies accompanied by mitochondrial disease. If clinical symptoms of muscle diseases sufficiently suggest mitochondrial abnormalities in the muscle, modified Gomori trichrome staining of a muscle biopsy sample may reveal ragged-red fibers (RRFs) and abnormal mitochondria accumulation. This morphologic identification can be confirmed biochemically by staining for succinate dehydrogenase and cytochrome c oxidase (COX), enzymes specific for mitochondria. In contrast, no specific clinical symptom pointing to mitochondrial nephropathy is known. Particularly the case absence for typical symptoms of "mitochondrial myopathy,

encephalopathy, lactic acidosis, and stroke-like episodes" (MELAS) often reveal only deafness or diabetes mellitus (DM) as the clinical symptom of mitochondrial disease.[12] Furthermore, for a diagnosis of isolated kidney disease with mitochondrial abnormalities, for example, FSGS, genetic mitochondrial analysis is started by a suspicion from kidney histology. Presently, morphologic evidence for mitochondrial abnormalities is assessed by electron microscopy with marked increase of abnormal-shaped mitochondria in podocytes or tubular epithelial cells.[5,12,14] However, sampling error for electron microscopic material may greatly affect the finding of sporadic abnormal cells, and thus, identifying abnormal cells by light microscopy may be helpful.

We have noted, but not proven, that the abnormal morphology in the tubular cells of mitochondrial nephropathies is distinguished by the presence of numerous mitochondria under a light microscope (Figs. 1, 2). We defined these abnormal epithelial cells, seen especially in distal tubuli and collecting ducts, as granular swollen epithelial cells (GSECs). In this study, we analyzed the presence of GSECs in various mitochondrial nephropathies that had already been diagnosed by genetic examinations of blood or skeletal muscle, and investigated the association between GSECs and clinical or histologic findings. In addition, we measured the mutant load of GSECs to determine whether GSECs are an abnormal cell with mutant mtDNA accumulation, similar to RRFs in skeletal muscle, using a single-cell PCR analysis.

Our data suggest that GSECs, primarily in the distal tubuli or collecting ducts, have distinct morphologic features suggesting mitochondrial nephropathy and are a useful tool in identifying secondary FSGS with mitochondrial abnormalities.

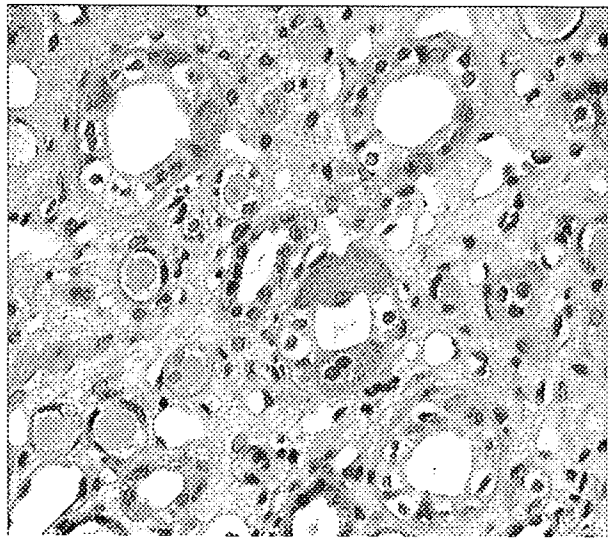

**FIGURE 1.** Light microscopic view of the granular swollen epithelial cell (GSEC). Arrows show GSECs in the collecting ducts (Masson trichrome stain × 200).

## MATERIALS AND METHODS

### Pathologic Analyses

We analyzed 7 biopsied kidneys from patients who had mtDNA position A3243G mutations and autopsied kidneys from 3 cases with T3271C mutations, including Kearns-Sayre syndrome, Pearson syndrome, and MELAS. Almost all biopsied patients were collected to our hospital (Kashiwa Hospital, The Jikei University School of Medicine, Chiba, Japan) for the diagnostic consultation from 7 institutions. Seven hundred ten kidney biopsies were analyzed between January 2001 to November 2009 and 15 patients were diagnosed as primary FSGS in our hospital. Among them, 1 patient (Patient 2) was FSGS related to genetically proven mitochondrial disease according to the finding of GSEC. Disease controls were randomly sampled 10 cases of IgA nephropathy (10 cases), primary FSGS (10 cases), and acute tubulointerstitial nephritis (10 cases). Formalin-fixed paraffin sections were stained with hematoxylin and eosin (HE), Masson trichrome, periodic acid-Schiff, and periodic-acid methenamine silver (PAM). A GSEC was defined as a granular swollen single epithelial cell in collecting ducts or distal tubuli. Masson trichrome stain is the best way to detect GSEC and PAM stain is suitable to distinguish GSEC from protein droplets in cases with proteinuria because the absorptive protein droplets are positive for PAM but not GSEC. We classified the extent of GSECs on the basis of the maximum number of GSECs in cross sections of collecting ducts or distal tubuli in a square high-power (× 400) field for 20 fields: mild = 1 to 2 cells, moderate = 3 to 5 cells, and severe = > 5 cells. Other histologic findings, including interstitial fibrosis or tubular atrophy and arteriolar hyalinosis, were classified using the Banff classification for transplanted kidneys.[22] Electron microscopic analysis was carried out in 5 biopsied cases (Patients 1 to 5).

### Measurements of mtDNA Mutant Loads in GSECs by Single-cell PCR Analysis

Paraffin-embedded kidney tissue from an autopsied case with a T3271C mutation was cut into 4-μm sections and stained with HE. After dehydration, we dissected each of 20 GSECs and normal-appearing epithelial cells from collecting ducts using a LM200 laser microdissection system (Arcturus Engineering Inc., Mountain View, CA). A PicoPure DNA Extraction Kit (Arcturus) was used to take out DNA from individually dissected cells. PCR amplification (30 s at 94°C, 30 s at 50°C, 30 s at 72°C, for 30 cycles) was carried out with a forward primer (5′-GGCAGAGCCCGGTAATC-3′: 3238 to 3254) and a reverse primer (5′-TAAGAAGAGGAATTGAACCTC TGACCTTAA-3′: 3272 to 3301) using an ABI 9700 thermal cycler (Applied Biosystems, Foster City, CA). PCR products were digested with AflII (Takara, Tokyo, Japan) for 24 hours, and restriction fragments (30 and 34 bp) were detected on 4% agarose gel (NuSieve 3:1

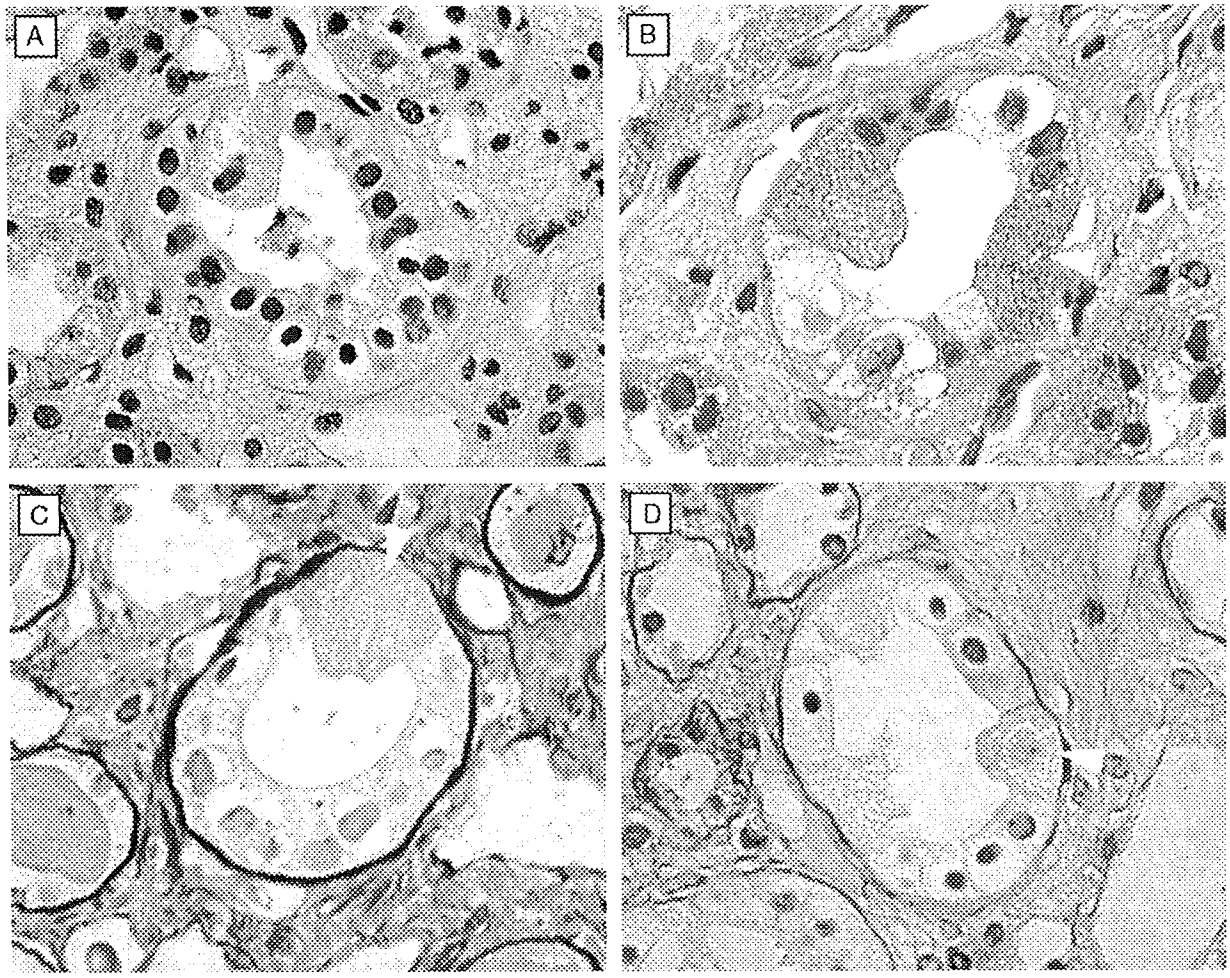


**FIGURE 2.** Higher magnification views of granular swollen epithelial cell (GSEC) by light microscopy. Arrowheads show GSECs in the collecting duct. (A) hematoxylin and eosin (HE) stain, (B) Masson trichrome stain, (C) periodic-acid methenamine (PAM) stain, (D) periodic acid-Schiff stain ( × 600).

Agarose; Lonza Rockland Inc., Rockland, ME). This PCR method was described earlier.[9,19] To measure the mutant load, the intensity of a fragment was determined using LabWorks (Bio Medical Equipment Service Co., Louisville, KY). A standard curve was constructed using a series of plasmid DNAs of known mutant proportions.

### Data Analysis

Data are presented as means ± SD. Mutant load groups were compared using the Mann-Whitney *U* test. The comparison of clinical and histopathologic findings among the groups was evaluated by Kruskal-Wallis test and Sheffe F-test. Correlations were analyzed using Spearman rank test. Data were analyzed using GraphPad Prism ver. 5.01. *P* values $< 0.05$ were deemed to indicate statistical significance.

## RESULTS

### Clinical Characteristics

The clinical characteristics of patients are shown in Tables 1 to 3. Biopsied patients with mtDNA A3243G mutation consisted of 5 female and 2 male patients: their mean age, mean serum Cr level, and mean proteinuria were 19.7 years, 0.81 mg/dL, and 1.87 g/d, respectively. Only 1 patient (Patient 2) exhibited nephrotic syndrome. Renal function was impaired in 2 cases (Patients 3 and 5). Serum levels of sodium, potassium, calcium, and phosphate were all normal. Renal tubular acidosis was not seen in any case. DM was identified in 3 cases (Patients 2, 3, and 5). Five patients (Patients 1, 2, 4, 5, and 7) had deafness. The mother of Patient 1 had received peritoneal dialysis for chronic renal failure of unknown origin. The mothers of Patients 2, 3, and 7 had DM. The younger brother of Patient 1 and the mother of Patient 6 also had A3243G mutations.

**TABLE 1.** Clinical Characteristics of Biopsied Patients With mtDNA A3243G Mutations

| Patient no. | Age (y)/Gender | s-Cr (mg/dL) | Ccr (mL/min) | Proteinuria (g/d) | Complications, Symptoms | Outcome of the Kidney |
|---|---|---|---|---|---|---|
| 1 | 14/F | 0.7 | 125 | 2.0 | Deafness | Dialysis |
| 2 | 25/F | 0.5 | 115 | 4.0 | DM, deafness | Renal insufficiency |
| 3 | 22/F | 1.6 | 30.8 | 0.9 | DM | Transplantation |
| 4 | 25/F | 0.6 | 73.3 | 2.3 | Deafness | Dialysis |
| 5 | 35/M | 1.5 | 45.9 | 0.5 | DM, deafness | Renal insufficiency |
| 6 | 12/F | 0.6 | 97.6 | 1.6 | None | Unknown |
| 7 | 5/M | 0.2 | 166 | 1.8 | Deafness | Unknown |

**TABLE 2.** Clinical Characteristics of Autopsied Patients

| Patient no. | Age (y)/Gender | Original Disease | Complications of the Kidney | Other Complications, Symptoms |
|---|---|---|---|---|
| 8 | 20/F | KSS (mtDNA deletion) | Fanconi syndrome chronic renal failure | Retinitis pigmentosa, DM, deafness, atrioventricular block, muscle weakness |
| 9 | 10/F | Pearson syndrome (mtDNA deletion) | Chronic renal failure | DM, muscle weakness, pancreatic insufficiency |
| 10 | 36/F | MELAS (T3271C mutation) | Acute renal failure | Stroke-like episodes, DM, muscle weakness |

KSS indicates Kearns-Sayre syndrome.

**TABLE 3.** Clinical Backgrounds of the Control Groups and Biopsied Patients With mtDNA A3243G Mutation

| | IgA Nephropathy (n = 10) | Primary FSGS (n = 10) | TIN (n = 10) | Biopsied Patients With A3243G Mutation (n = 7) |
|---|---|---|---|---|
| Male/Female | 5/5 | 7/3 | 3/7 | 2/5 |
| Age (y) | 37.7 ± 17.2 | 42.5 ± 12.5 | 45.3 ± 28.5 | 19.7 ± 10.0 |
| s-Cr (mg/dL) | 0.76 ± 0.24 | 1.07 ± 0.57 | 2.81 ± 2.19* | 0.81 ± 0.53 |
| Proteinuria (g/d) | 0.75 ± 0.36 | 6.10 ± 3.04† | 0.50 ± 0.45 | 1.87 ± 1.23 |

*$P < 0.05$, versus IgA nephropathy, primary FSGS and biopsied patients with A 3243G mutation.
†$P < 0.01$, versus IgA nephropathy, TIN and biopsied patients with A 3243G mutation.
FSGS indicates focal segmental glomerulosclerosis; TIN, tubulointerstitial nephritis.

**TABLE 4.** Histopathologic Findings

| Patient no. | GSEC | Global Sclerosis (%) | FSGS Lesion (%) | IF/TA | Arteriolar Hyalinosis |
|---|---|---|---|---|---|
| 1 | Mild | 0/6 | 1/6 (16.7) | Mild | Mild |
| 2 | Moderate | 3/10 (30) | 1/10 (10) | Moderate | Moderate |
| 3 | Moderate | 3/28 (10.7) | 11/28 (39.2) | Moderate | Mild |
| 4 | Moderate | 6/48 (12.5) | 4/48 (8.3) | Mild | Mild |
| 5 | Moderate | 1/12 (8.3) | 1/12 (8.3) | Mild | Mild |
| 6 | Moderate | 3/10 (30) | 1/10 (10) | Mild | None |
| 7 | Mild | 3/12 (25) | 1/12 (8.3) | Mild | Moderate |
| 8 | Mild | 196/283 (69.2) | 12/283 (4.2) | Severe | Severe |
| 9 | Severe | 156/234 (66.6) | 3/234 (1.3) | Severe | Mild |
| 10 | Severe | 8/362 (2.2) | 0/362 | None | None |

FSGS indicates focal segmental glomerulosclerosis; IF/TA, interstitial fibrosis and tubular atrophy.

All autopsied cases were female and they all had DM. The patient with Kearns-Sayre syndrome had Fanconi syndrome and chronic renal failure, and the patient with Pearson syndrome also had chronic renal failure. The patient having MELAS with a T3271C mutation had episodes of acute renal failure.

## Histopathologic Findings

Histologic findings are summarized in Tables 4 and 5. Various extents of tubulointerstitial fibrosis and tubular atrophy were observed in 9 patients. GSECs were recognized in all patients, but no case of IgA nephropathy, primary FSGS, or acute tubulointerstitial nephritis

**TABLE 5.** Histopathologic Findings of the Control Groups and Biopsied Patients With mtDNA A3243G Mutation

| | IgA Nephropathy (n = 10) | Primary FSGS (n = 10) | TIN (n = 10) | Biopsied Patients With A3243G Mutation (n = 7) |
|---|---|---|---|---|
| GS (%) | 10.0 ± 8.17 | 1.61 ± 2.13 | 4.17 ± 6.13 | 16.6 ± 11.7* |
| FSGS lesion (%) | 1.61 ± 2.13 | 13.2 ± 9.60** | 0.71 ± 2.24 | 14.4 ± 11.3† |
| IF/TA | 0.30 ± 0.48 | 0.30 ± 0.48 | 0.70 ± 0.82 | 1.29 ± 0.48‡ |
| ah | 0.40 ± 0.69 | 0.60 ± 0.69 | 0.60 ± 0.48 | 1.14 ± 0.69 |
| GSEC | 0 | 0 | 0 | 1.71 ± 0.48§ |

IF/TA, ah and GSEC are shown as the mean score of the grades (1: mild, 2: moderate, 3: severe).
*$P < 0.05$, versus Primary FSGS and TIN.
†$P < 0.05$, versus IgA nephropathy and TIN.
‡$P < 0.05$, versus IgA nephropathy and Primary FSGS.
§$P < 0.01$, versus IgA nephropathy, Primary FSGS and TIN.
ah indicates arteriolar hyalinosis; FSGS, focal segmental glomerulosclerosis; GS, global sclerosis; GSEC, glanular swollen epithelial cell; IF/TA, interstitial fibrosis and tubular atrophy; TIN, tubulointerstitial nephritis.

was observed. Electron micrographs from 5 patients (Patients 1 to 5) also showed epithelial cells with increased numbers of mitochondria in the distal tubuli (Figs. 3A, B), some of which had coil-like arranged cristae (Fig. 3B, inset). Although the accumulation of abnormal mitochondria was sometimes seen in proximal tubuli by electron microscopy, it is difficult to identify by light microscopy, probably because abundant cytoplasma and osmiophilic features in normal proximal tubular epithelium are hard to distinguish and even abnormal mitochondria is increased. Electron microscopic views showed mosaic patterns consisting of mitochondria-abundant epithelial cells and normal-appearing epithelial cells in the same cross sections of distal tubuli (Fig. 3A).

Regarding glomerular lesions, FSGS lesions were observed in 9 patients. Electron microscopy revealed podocytes containing marked proliferating and irregular mitochondria in 4 patients who had FSGS lesions.

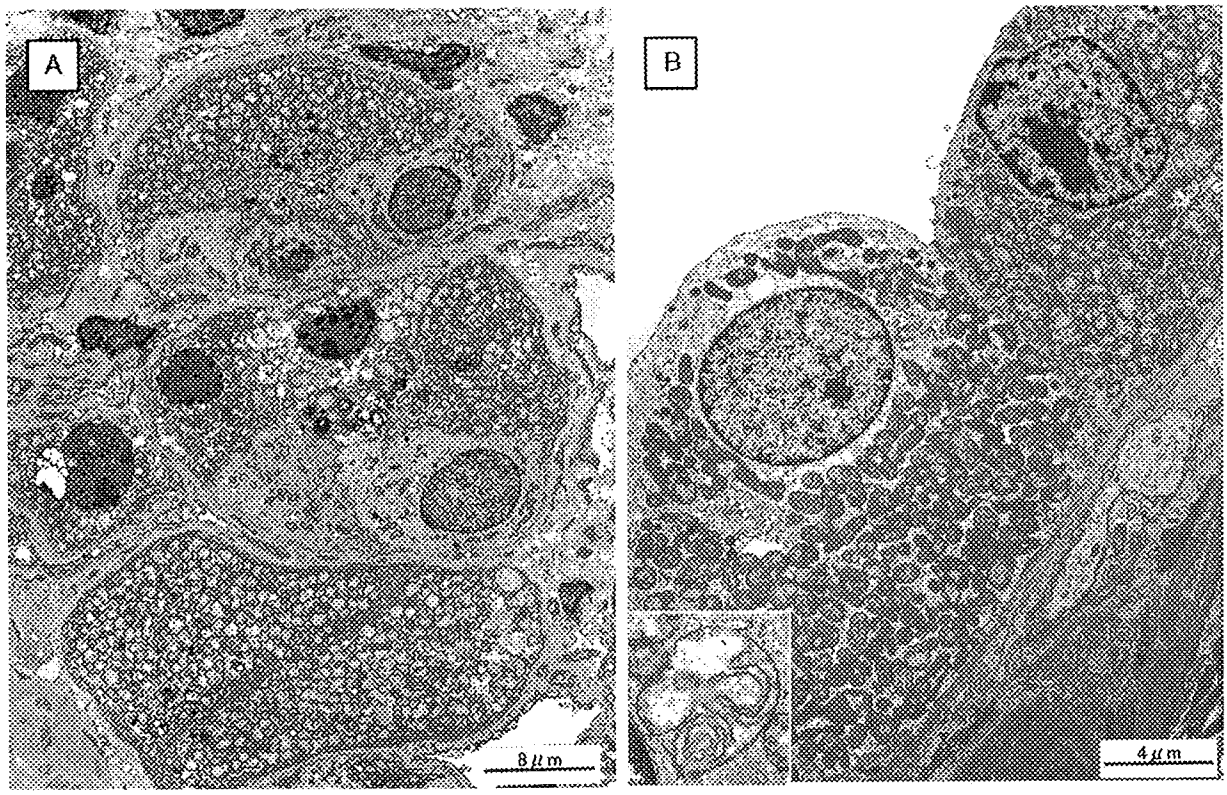


**FIGURE 3.** Electron microscopic views of the distal tubuli. A, A mosaic pattern consisting of mitochondria-abundant epithelial cells and normal-appearing epithelial cells is recognized in the distal tubules ( × 1500). B, High magnification of the distal tubular epithelial cell reveals a markedly increased number of mitochondria ( × 3000) and some of which were coil-like arranged cristae (inset, × 40,000).

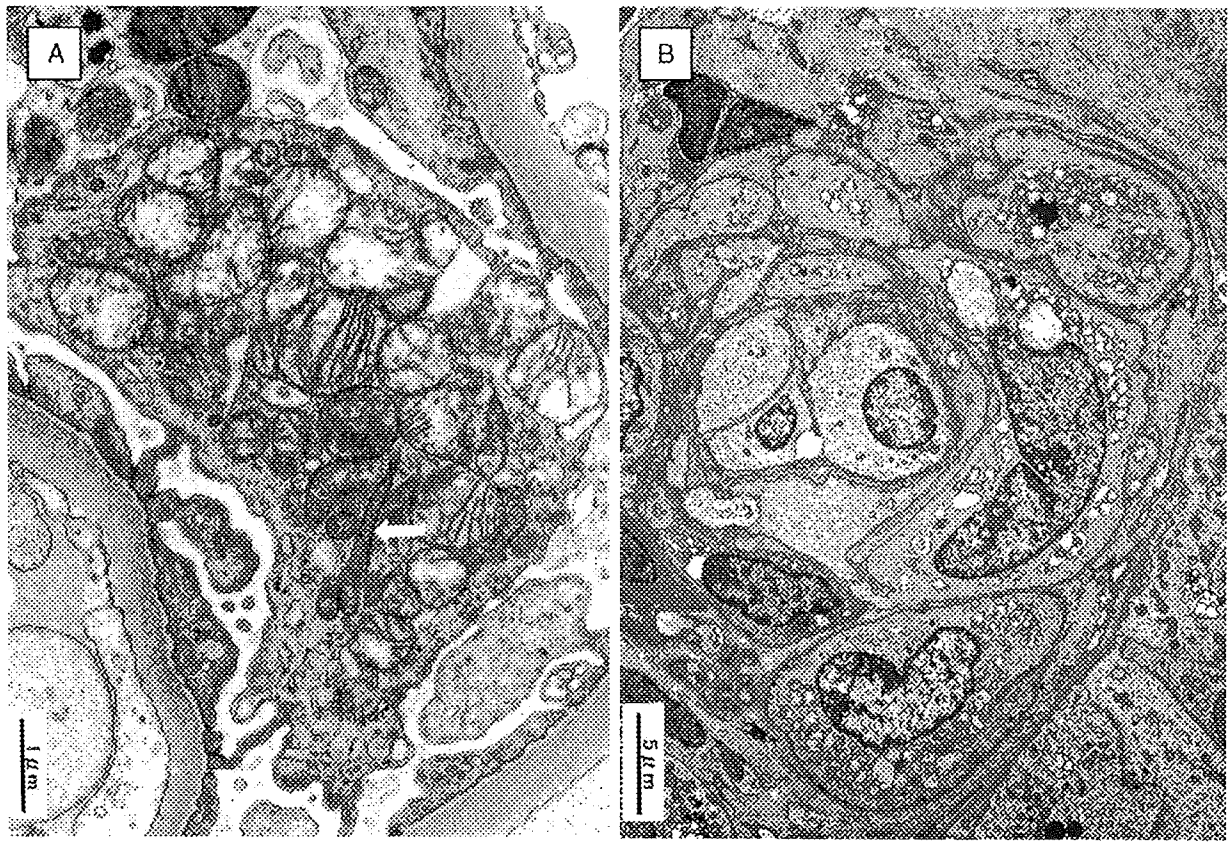


FIGURE 4. Electron microscopic views of a podocyte and an arteriole in Patient 3. A, Abnormal mitochondria increased in a podocyte. The size and shape of mitochondria are irregular, including swollen and ballooning mitochondria. One of these has a unicorn-shaped giant mitochondria (arrow; × 5000). B, Increased number of mitochondria in arteriolar smooth muscles (× 2000).

The size and shape of the mitochondria were irregular, including swollen and ballooning mitochondria (Fig. 4A). Of these, 1 had a "unicorn-shaped" giant mitochondria (Fig. 4A, arrow).

Concerning vascular lesions, arteriolar hyalinosis was identified in 8 patients. Patient 3 showed increased numbers of mitochondria in arteriolar smooth muscle cells on the basis of electron microscopy (Fig. 4B).

### The Grade of GSECs and Clinical or Pathologic Parameters

No significant correlation was observed between the grade of GSECs and renal function, including serum Cr levels and proteinuria. Histologically, the grade also did not correlate with the score of interstitial fibrosis and tubular atrophy, arteriolar hyalinosis, or the proportion of global or focal segmental sclerosis (Fig. 5).

### Mitochondrial DNA Mutant Loads in GSECs

A DNA sample from each microdissected GSEC was amplified by PCR and digested with AflII. Two cleaved fragments (34 and 30 bp) were detected (Fig. 6A). The mutant load of GSECs was significantly higher than in normal-appearing epithelial cells (Fig. 6B; 63.4 ± 17.8% vs. 32.5 ± 4.6%, $P < 0.0001$).

## DISCUSSION

Cells with mitochondrial abnormalities have been identified at the ultrastructural level, revealing the accumulation of morphologically abnormal mitochondria within the cytoplasm. The abnormal cells reported in mitochondrial nephropathy are often present in tubular cells and podocytes[5,8,12,14,21] as seen during electron microscopy. As the distribution of abnormal cells in situ is sporadic rather than ubiquitous, identifying them by light microscopy within this tissue may be useful for the diagnosis of mitochondrial nephropathy.

We found mitochondrial-rich cells among tubular epithelial cells by Masson trichrome staining and noted that the accumulation of mitochondria in these cells may indicate mitochondrial abnormalities.

As shown in Figures 1 and 2 single expanded epithelial cells among tubular cells were fully stained by Masson trichrome staining, suggesting mitochondrial

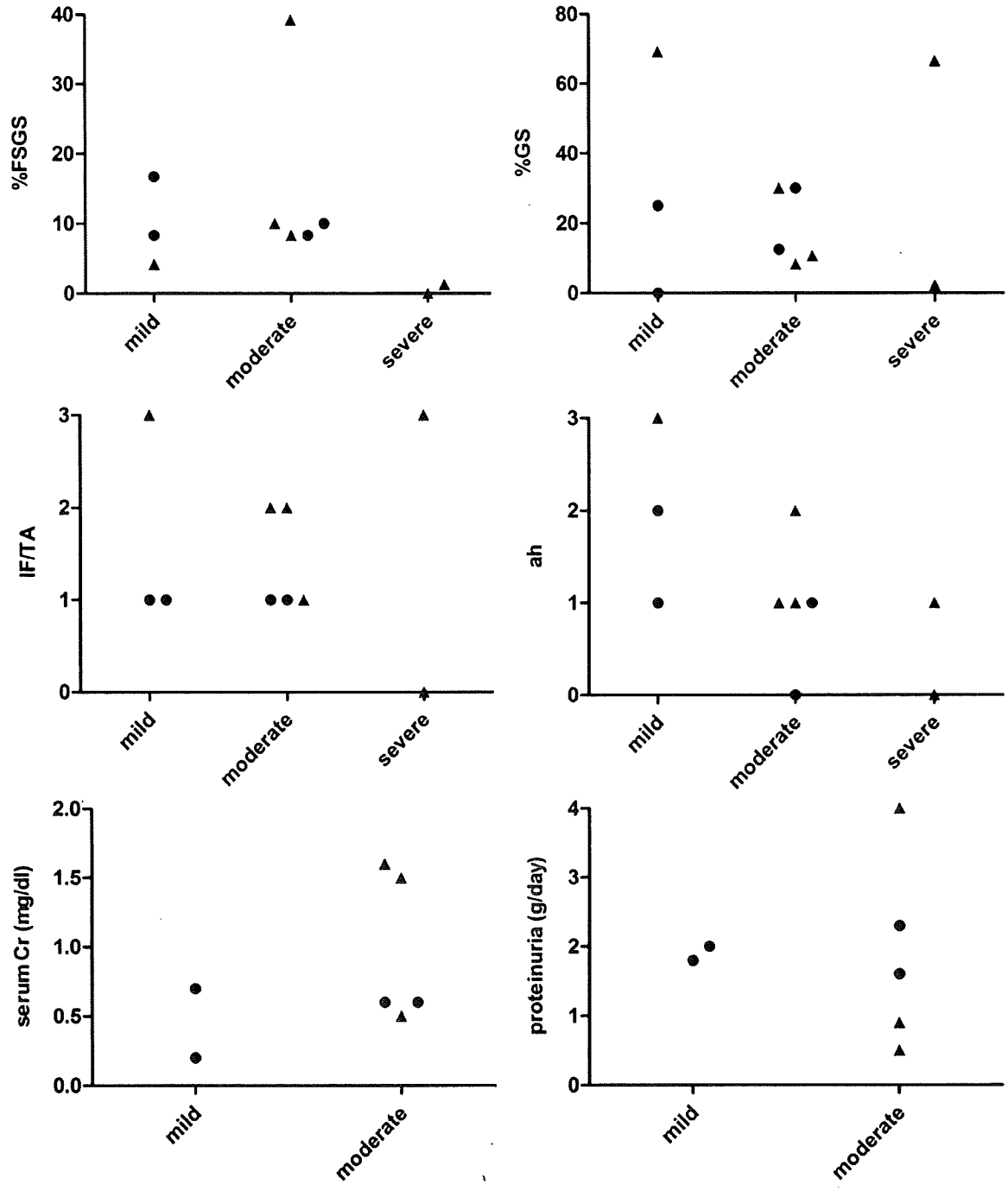


**FIGURE 5.** The association between the granular swollen epithelial cell (GSEC) grade (x-axis) and pathologic or clinical parameters (y-axis). ah indicates arteriolar hyalinosis; % focal segmental glomerulosclerosis (FSGS), proportion of focal segmental glomerulosclerosis; %GS, proportion of global sclerosis; IF/TA, interstitial fibrosis, and tubular atrophy. The grades of IF/TA and ah were classified as: 1, mild; 2, moderate; 3, severe. Clinical data of serum Cr and proteinuria were obtained from biopsied patients (n = 7). ▲: Diabetes mellitus (DM) patients. Serum Cr and proteinuria in patients of autopsy cases were omitted (n = 3).

proliferation. These cells indeed showed accumulation of morphologically abnormal mitochondria (Fig. 3).

In this study, we examined 10 cases with genetically proven mitochondrial disease and found that GSECs were present in all kidney samples obtained by biopsy or autopsy.

GSECs were recognized not only in patients with the A3243G mutation, but also in patients with some

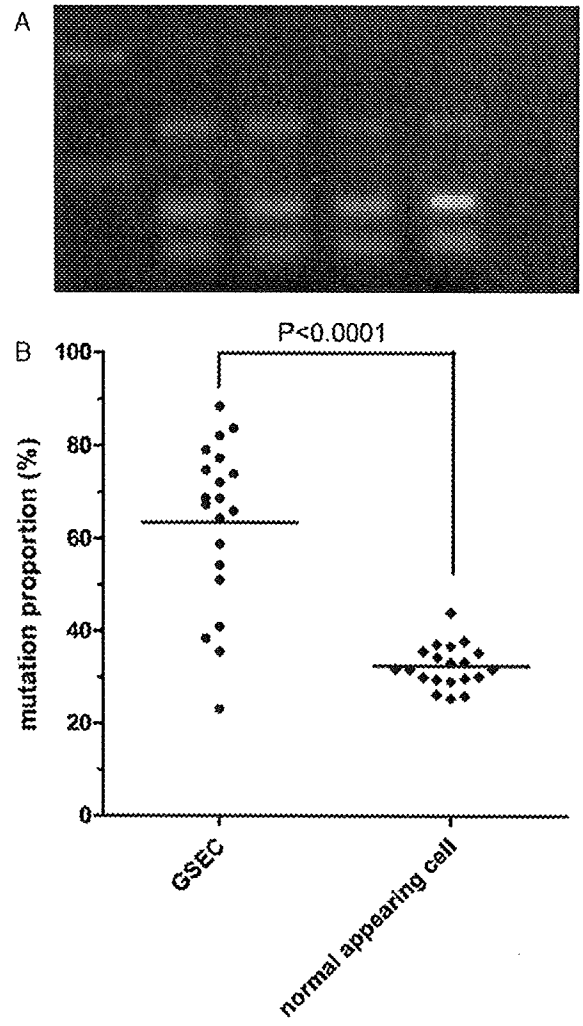


**FIGURE 6.** Identification of the T3271C mutation and comparisons of the mutant loads in granular swollen epithelial cell (GSECs) and normal-appearing epithelial cells. A, Each lane showed the results of PCR amplification from a single GSEC. DNA samples from each microdissected GSEC were amplified by PCR and digested with AflII. Two cleaved fragments (34 and 30 bp) were detected. B, The mutant load in GSECs was significantly higher than in normal-appearing epithelial cells (63.4 ± 17.8% vs. 32.5 ± 4.6%; $P < 0.0001$).

mitochondrial diseases. Thus, GESCs may not reflect specific genetic mitochondrial abnormalities. We found no GSECs in specimens from cases of IgA nephropathy, primary FSGS, or acute tubulointerstitial nephritis, suggesting that such epithelial features may be related to mitochondrial nephropathy.

To define whether morphologically determined GSECs really had mitochondrial mutations, we measured the mutant load of GSECs and normal-appearing epithelial cells from the collecting duct by single-cell PCR analysis using each GSEC that was laser-microdissected from paraffin-embedded kidney tissue. For this procedure, we modified the single-fiber PCR analysis earlier used for RRFs in cases of MELAS.[17] As biopsy samples contain few GSECs, we applied this method to autopsy samples from a patient who had MELAS with a T3271C mtDNA mutation. We found a higher mutant load in GSECs than in normal-appearing cells, indicating that the GSECs represent mutant mitochondria accumulation, similar to that of RRFs in skeletal muscle. This is consistent with earlier studies reporting that the proportion of mutant mtDNA was higher in RRFs than in non-RRFs in muscle.[16,17] Simultaneously, we identified a few GSECs with low mutant loads. As shown in Figure 6, about 20% of GSECs showed low mutant loads. The reason for this phenomenon is unclear, but it may be argued that RRFs often maintain COX activity in patients with MELAS. Moreover, these COX-positive RRFs show that mitochondrial proliferation is not always an unsuccessful response to mitochondrial dysfunction. Extensive normal mitochondrial proliferation can provide functional compensation.[17]

Although GSECs indicate mtDNA mutations in kidney-resident cells, whether GSECs cause tissue damage resulting from FSGS or Fanconi syndrome is not known. Notably, the grade of GSECs did not correlate with percent FSGS. This is not inconsistent because mitochondrial abnormalities occur in a cell-specific manner and the frequency of GSECs in tubular cells does not necessarily correlate with FSGS caused by podocyte dysfunction, as shown by abnormal mitochondria in podocytes.[12] Yamagata et al showed that a common mtDNA deletion was observed primarily in glomerular epithelial cells using in situ PCR analysis, and they suggested the possibility that this mtDNA deletion may be the cause of glomerular epithelial damage.[23] Indeed, 4 of the 5 cases in this study in which electron microscopy was carried out showed that podocytes also contained proliferating abnormal mitochondria. In this context, we did not notice apparent GSECs in podocytes in cases with FSGS. Although the reason is unknown, podocytes may show a variety of morphologies with large and loose cytoplasm, and thus features of GSECs seen in the tubular cells are hard to detect in the case of podocytes. Other histologic parameters (IF/TA, percent GS, arteriolar hyalinosis) and clinical parameters (serum Cr levels, proteinuria) did not correlate with the grade of GSEC. This may have occurred because the proportion of mutant mtDNA varies in different cell types owing to the heteroplasmic character of mitochondrial disease and because the tissue injury depends on the damaged cells. Nakada et al showed that in mice with mutant mtDNA carrying a 4696-bp deletion (⊿mtDNA4696), the appearance of COX-negative mitochondria was limited to tissues with more than 85% ⊿mtDNA4696, and that it was correlated with the onset of disease phenotypes.[18] For our patients, functional abnormalities might not have occurred because the mutant load was not sufficiently high in the GSECs and the number of GSECs was limited.

An example in which cells with abnormal mitochondria directly cause tissue damage is seen in the mitochondrial morphologic abnormalities in arteriolar smooth muscle cells. Patients 1, 4, and 7 showed arteriolar hyalinosis without having DM. Earlier reports have shown arteriolar lesions similar to those in our cases.[6,11] Arteriolar hyalinosis in non-DM-associated mitochondrial nephropathy shows arteriolar smooth muscle cells containing marked proliferating mitochondria. This may be a background of mitochondrial abnormality-induced arteriolar changes.

In conclusion, we showed that GSECs in kidney tissue may represent abnormal mitochondrial accumulation, as revealed by the high mutant load using PCR. This suggests that GSECs may become a new diagnostic marker to identify secondary FSGS associated with mitochondrial diseases and that it may be useful in avoiding unnecessary noneffective therapy, such as steroids in FSGS.

## ACKNOWLEDGMENTS

*The authors thank Dr Makoto Ogura, Kashiwa Hospital, The Jikei University School of Medicine, Dr Kosaku Nitta, Tokyo Women's Medical University, Dr Kenjiro Kimura, Dr Junki Koike, St. Marianna University School of Medicine, Dr Mikiya Fujieda, Kochi University, and Dr Kunimasa Yan, Kyorin University, for providing samples of renal biopsies. We also thank Shigeru Horita, Mayuko Ohno, Tokyo Women's Medical University, and Sachiko Ishii, Kashiwa Hospital, The Jikei University School of Medicine, for their support in pathologic analyses. In addition, we thank Mayuko Kato, National Center of Neurology and Psychiatry, for providing technical support during single-cell PCR analysis.*

## REFERENCES

1. Adedoyin O, Frank R, Vento S, et al. Cardiac disease in children with primary glomerular disorders—role of focal segmental glomerulosclerosis. *Pediatr Nephrol.* 2004;19:408–412.
2. Au KM, Lau SC, Mak YF, et al. Mitochondrial DNA deletion in a girl with Fanconi's syndrome. *Pediatr Nephrol.* 2007;22:136–140.
3. D'Agati VD. The spectrum of focal segmental glomerulosclerosis: new insights. *Curr Opin Nephrol Hypertens.* 2008;17:271–281.
4. DiMauro S, Bonilla E, Zeviani M, et al. Mitochondrial myopathies. *Ann Neurol.* 1985;17:521–538.
5. Dinour D, Mini S, Polak-Charcon S, et al. Progressive nephropathy associated with mitochondrial tRNA gene mutation. *Clin Nephrol.* 2004;62:149–154.
6. Doleris LM, Hill GS, Chedin P, et al. Focal segmental glomerulosclerosis associated with mitochondrial cytopathy. *Kidney Int.* 2000; 58:1851–1858.
7. Egger J, Lake BD, Wilson J. Mitochondrial cytopathy. A multisystem disorder with ragged red fibres on muscle biopsy. *Arch Dis Child.* 1981;56:741–752.
8. Goto Y, Itami N, Kajii N, et al. Renal tubular involvement mimicking Bartter syndrome in a patient with Kearns-Sayre syndrome. *J Pediatr.* 1990;116:904–910.
9. Goto Y, Nonaka I, Horai S. A new mtDNA mutation associated with mitochondrial myopathy, encephalopathy, lactic acidosis and stroke-like episodes (MELAS). *Biochim Biophys Acta.* 1991; 1097:238–240.
10. Güçer S, Talim B, Aşan E, et al. Focal segmental glomerulosclerosis associated with mitochondrial cytopathy: report of two cases with special emphasis on podocytes. *Pediatr Dev Pathol.* 2005;8: 710–717.
11. Hasegawa H, Matsuoka T, Goto Y, et al. Strongly succinate dehydrogenase-reactive blood vessels in muscles from patients with mitochondrial myopathy, encephalopathy, lactic acidosis, and stroke-like episodes. *Ann Neurol.* 1991;29:601–605.
12. Hotta O, Inoue C, Miyabayashi S, et al. Clinical and pathologic features of focal segmental glomerulosclerosis with mitochondrial tRNALeu (UUR) gene mutation. *Kidney Int.* 2001;59:1236–1243.
13. Kambham N, Markowitz GS, Valeri AM, et al. Obesity-related glomerulopathy: an emerging epidemic. *Kidney Int.* 2001;59: 1498–1509.
14. Löwik MM, Hol FA, Steenbergen EJ, et al. Mitochondrial tRNALeu (UUR) mutation in a patient with steroid-resistant nephrotic syndrome and focal segmental glomerulosclerosis. *Nephrol Dial Transplant.* 2005;20:336–341.
15. Mallick N. Secondary focal glomerulosclerosis not due to HIV. *Nephrol Dial Transplant.* 2003;18(suppl 6):vi64–vi67.
16. Mita S, Tokunaga M, Uyama E, et al. Single muscle fiber analysis of myoclonus epilepsy with ragged-red fibers. *Muscle Nerve.* 1998;21: 490–497.
17. Moraes C, Ricci E, Bonilla E, et al. The mitochondrial tRNA [Leu (UUR)] mutation in mitochondrial encephalomyopathy, lactic acidosis, and stroke-like episodes (MELAS): genetic, biochemical, and morphological correlations in skeletal muscle. *Am J Hum Gene.* 1992;50:934–949.
18. Nakada K, Inoue K, Ono T, et al. Inter-mitochondrial complementation: mitochondria-specific system preventing mice from expression of disease phenotypes by mutant mtDNA. *Nat Med.* 2001;7:934–940.
19. Nagashima T, Kato H, Maguchi S, et al. A mitochondrial encephalo-myo-neuropathy with a nucleotide position 3271 (T-C) point mutation in the mitochondrial DNA. *Neuromuscul Disord.* 2001;11:470–476.
20. Niaudet P, Rotig A. The kidney in mitochondrial cytopathies. *Kidney Int.* 1997;51:1000–1007.
21. Niaudet P, Heidet L, Munnich A, et al. Deletion of the mitochondrial DNA in a case of de Toni-Debré-Fanconi syndrome and Pearson syndrome. *Pediatr Nephrol.* 1994;8:164–168.
22. Solez K, Colvin RB, Racusen LC, et al. Banff '05 Meeting Report: differential diagnosis of chronic allograft injury and elimination of chronic allograft nephropathy ("CAN"). *Am J Transplant.* 2007; 7:518–526.
23. Yamagata K, Muro K, Usui J, et al. Mitochondrial DNA mutations in focal segmental glomerulosclerosis lesions. *J Am Soc Nephrol.* 2002;13:1816–1823.

# PDK1 coordinates survival pathways and β-adrenergic response in the heart

Kaoru Ito[a], Hiroshi Akazawa[a], Masaji Tamagawa[b], Kensuke Furukawa[c], Wataru Ogawa[c], Noritaka Yasuda[a], Yoko Kudo[a], Chien-hui Liao[a], Rie Yamamoto[a], Toshiaki Sato[b], Jeffery D. Molkentin[d], Masato Kasuga[c], Tetsuo Noda[e], Haruaki Nakaya[b], and Issei Komuro[a,1]

Departments of [a]Cardiovascular Science and Medicine and [b]Pharmacology, Chiba University Graduate School of Medicine, 1-8-1 Inohana, Chuo-ku, Chiba 260-8670, Japan; [c]Division of Diabetes, Metabolism, and Endocrinology, Department of Internal Medicine, Kobe University Graduate School of Medicine, 7-5-1 Kusunoki-cho, Chuo-ku, Kobe 650-0017, Japan; [d]Department of Pediatrics, University of Cincinnati, Children's Hospital Medical Center, 3333 Burnet Avenue, Cincinnati, OH 45229; and [e]Department of Cell Biology, Japanese Foundation for Cancer Research, Cancer Institute, 3-10-6 Ariake, Koto-ku, Tokyo 135-8550, Japan

Edited by Eric N. Olson, University of Texas Southwestern Medical Center, Dallas, TX, and approved April 2, 2009 (received for review January 5, 2009)

**The 3-phosphoinositide-dependent kinase-1 (PDK1) plays an important role in the regulation of cellular responses in multiple organs by mediating the phosphoinositide 3-kinase (PI3-K) signaling pathway through activating AGC kinases. Here we defined the role of PDK1 in controlling cardiac homeostasis. Cardiac expression of PDK1 was significantly decreased in murine models of heart failure. Tamoxifen-inducible and heart-specific disruption of *Pdk1* in adult mice caused severe and lethal heart failure, which was associated with apoptotic death of cardiomyocytes and $\beta_1$-adrenergic receptor (AR) down-regulation. Overexpression of Bcl-2 protein prevented cardiomyocyte apoptosis and improved cardiac function. In addition, PDK1-deficient hearts showed enhanced activity of PI3-K$\gamma$, leading to robust $\beta_1$-AR internalization by forming complex with $\beta$-AR kinase 1 ($\beta$ARK1). Interference of $\beta$ARK1/PI3-K$\gamma$ complex formation by transgenic overexpression of phosphoinositide kinase domain normalized $\beta_1$-AR trafficking and improved cardiac function. Taken together, these results suggest that PDK1 plays a critical role in cardiac homeostasis in vivo by serving as a dual effector for cell survival and $\beta$-adrenergic response.**

AGC kinase | apoptosis | heart failure | receptor internalization

Heart failure, a major cause of morbidity and mortality worldwide, is a clinical syndrome in which the heart is incapable of pumping blood at a rate commensurate with systemic demands (1). Injurious stresses from extrinsic or intrinsic origins trigger the complex intracellular signaling pathways in cardiomyocytes and thereby activate the compensatory mechanisms involving alterations in survival and growth signals, calcium handling, and energy production (2). Simultaneously, the sympathetic nervous, renin-angiotensin-aldosterone, and cytokine systems are activated to cope with a decline in cardiac performance. Although these compensatory systems initially maintain cardiac function within a physiological range, prolonged activation of these systems paradoxically leads to cardiac damage and worsens clinical prognosis (2). Therefore, for the elucidation of the pathophysiology of heart failure, it is very important to dissect the inherent complexity of intracellular signaling pathways that coordinate the cellular homeostasis and neurohumoral responses in cardiomyocytes.

The 3-phosphoinositide-dependent protein kinase-1 (PDK1) is a member of the AGC serine/threonine kinase family that functions downstream of phosphoinositide 3-kinase (PI3-K) and activates several AGC kinases, including Akt, p70 ribosomal S6 kinase (p70S6K), and serum- and glucocorticoid-induced protein kinase 1 (SGK1), by phosphorylating these enzymes at their activation loops (3). The physiological functions of PDK1 have been investigated by targeted disruption of *Pdk1* gene. Mouse embryos systemically deficient for *Pdk1* were lethal during early embryogenesis, displaying multiple abnormalities that included lack of somites, forebrain, and neural crest-derived tissues (4). Alessi et al. (5) recently generated striated muscle-specific PDK1 conditional knockout mice (PDK1-MCKCre) by crossing mice harboring a "floxed" *Pdk1* allele with transgenic mice expressing Cre recombinase under the control of the *muscle creatine kinase* (*MCK*) promotor. PDK1-MCKCre mice died of heart failure by 11 weeks of age. Interestingly, PDK1-MCKCre mice showed attenuation of cardimyocyte cell growth and impairment of left ventricular (LV) contraction. It was reported that cardiomyocytes deficient for *Pdk1* were sensitive to hypoxia (5), and that ischemic preconditioning failed to protect *Pdk1*-hypomorphic mutant mice against myocardial infarction (MI) (6). However, the mechanisms of how PDK1 deficiency induces these cardiac abnormalities remain to be resolved.

In this study, we found that the expression levels of PDK1 protein were significantly decreased in the failing hearts of murine models. We generated tamoxifen-inducible and heart-specific PDK1 conditional knockout mice (PDK1-MerCre) to elucidate the relevance of PDK1 to the pathogenesis of heart failure. We disrupted the *Pdk1* gene in the adulthood and demonstrated that PDK1 plays a role in the regulation of normal cardiac function by preventing cardiomyocyte apoptosis and by preserving responsiveness to $\beta$-adrenergic stimulation.

## Results

**Generation of Tamoxifen-Inducible and Heart-Specific PDK1 Knockout Mice.** We examined alterations in the expression levels of PDK1 in failing hearts. Heart failure was induced in mice by producing myocardial infarction or administering doxorubicin i.p. Two weeks after operation of myocardial infarction or doxorubicin injection, expression levels of PDK1 were significantly decreased in the failing hearts, compared with control hearts (Fig. S1).

To assess the pathophysiological significance of PDK1 down-regulation, we created a model of temporally regulated inactivation of *Pdk1* specifically in the adult hearts. We crossed *Pdk1*$^{flox/flox}$ mice (7, 8) with transgenic mice expressing tamoxifen-inducible Cre recombinase protein fused to two mutant estrogen-receptor ligand-binding domains (MerCreMer) under the control of the *α-myosin heavy chain* promoter (9). In the resulting *Pdk1*$^{flox/flox}$/*MerCreMer*$^{+}$ mice (PDK1-MerCre) at the age of 10 weeks, we administered tamoxifen successively for 5 days and confirmed by immunoblot analysis that functional PDK1 expression was almost undetectable specifically in the hearts on day 7 after the initiation of tamoxifen treatment (Fig. S2*A*).

Next, we examined whether the activation of kinases downstream of PDK1 were suppressed in the hearts of PDK1-MerCre. In

Author contributions: H.A. and I.K. designed research; K.I., M.T., K.F., N.Y., Y.K., C.-h.L., and R.Y. performed research; K.F., J.D.M., and T.N. contributed new reagents/analytic tools; K.I., M.T., W.O., T.S., M.K., and H.N. analyzed data; and K.I., H.A., and I.K. wrote the paper.

The authors declare no conflict of interest.

This article is a PNAS Direct Submission.

[1]To whom correspondence should be addressed. E-mail: komuro-tky@umin.ac.jp.

This article contains supporting information online at www.pnas.org/cgi/content/full/0900064106/DCSupplemental.

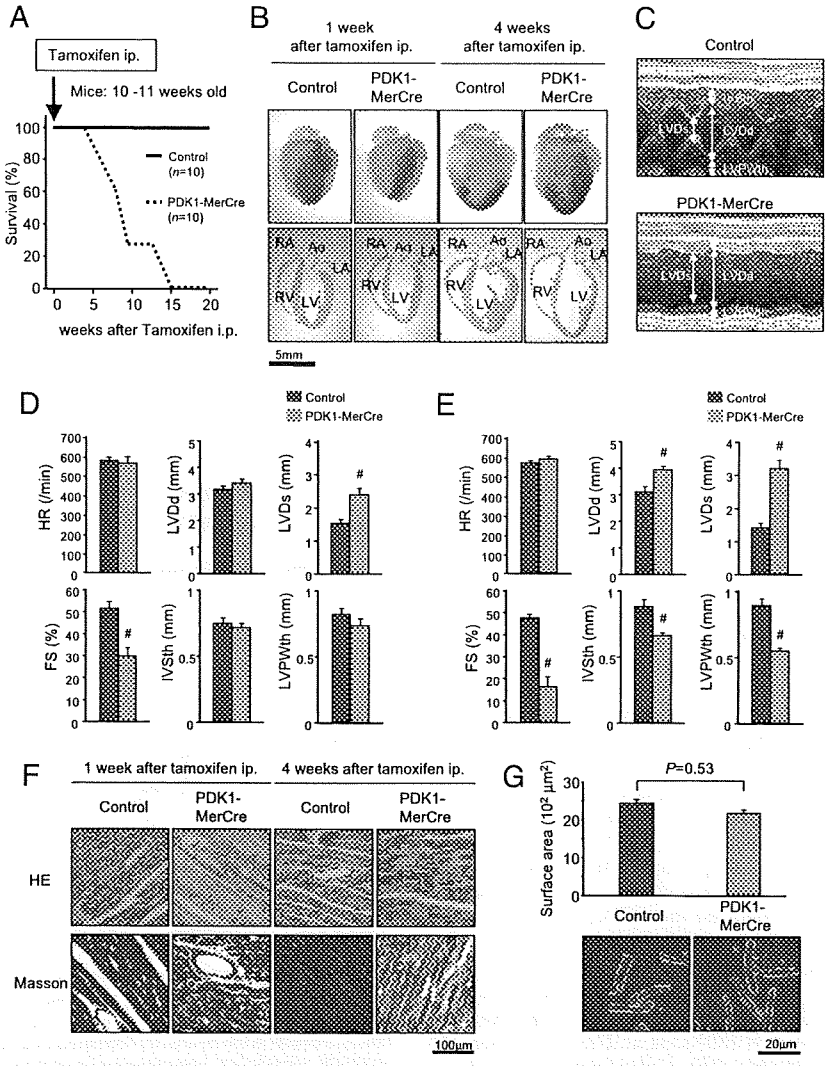


**Fig. 1.** Severe heart failure observed in PDK1-MerCre mice. (*A*) Kaplan-Meier survival curves of PDK1-MerCre mice (n = 10) and control mice (n = 10). Mice were injected with tamoxifen at the age of 10–11 weeks. (*B*) Macroscopic findings and 4-chamber sections of the hearts from PDK1-MerCre and control mice 1 and 4 weeks after the initiation of tamoxifen treatment. Ao, aorta; LA, left atrium; LV, left ventricule; RA, right atrium; RV, right ventricule. (*C*) Representative M-mode echocardiograms of mice 1 week after tamoxifen treatment. (*D*) Echocardiographic measurements of PDK1-MerCre and control mice 1 week after tamoxifen treatment. HR, heart rate; LVDd, LV dimension in diastole; LVDs, LV dimension in systole; FS, fractional shortening; IVSth, interventricular septum thickness; LVPWth, LV posterior wall thickness. Values represent the mean ± SEM of data from 10 mice in each group. #, $P < 0.01$ versus control group. (*E*) Echocardiographic measurements of PDK1-MerCre and control mice 4 weeks after tamoxifen treatment. Values represent the mean ± SEM of data from 6 mice in each group. #, $P < 0.01$ versus control group. (*F*) Histological sections with hematoxylin and eosin (HE) staining and Masson's trichrome (Masson) staining of PDK1-MerCre and control mice 1 and 4 weeks after tamoxifen treatment. (*G*) Surface areas of isolated cardiomyocytes (57 individual cardiomyocytes in each group) and sample pictures of isolated cardiomyocytes from PDK1-MerCre and control mice 1 week after tamoxifen treatment. Values represent the mean ± SEM.

mammalian cells, Akt is fully activated through PDK1-dependent phosphorylation of Thr-308 and PDK1-independent phosphorylation of Ser-473 (10). Insulin-induced phosphorylation of Akt at Thr-308 in PDK1-MerCre hearts was significantly attenuated, compared with control hearts, while phosphorylation level at Ser-473 was unchanged (Fig. S2*B*). As a consequence, Akt kinase activity was markedly reduced in PDK1-MerCre hearts (Fig. S2*C*). Consistently, insulin-induced phosphorylation levels of glycogen synthase kinase (GSK) 3$\beta$ at Ser-9, mammalian target of rapamycin (mTOR) at Ser-2448, and p70S6K at Thr-389 (11) were attenuated in the PDK1-MerCre hearts (Fig. S2*B*). Collectively, these results indicate that Akt signaling is inhibited in PDK1-MerCre hearts.

**Lethal Heart Failure in PDK1-MerCre Mice.** Without tamoxifen treatment, PDK1-MerCre mice survived normally and were indistinguishable in appearance from control littermates. Strikingly, all PDK1-MerCre mice died from 5 to 15 weeks after the initiation of tamoxifen treatment (Fig. 1*A*).

One week after tamoxifen treatment, cardiac sizes were not significantly different between PDK1-MerCre mice and control mice (Fig. 1*B*). Echocardiographic examination revealed a significant decrease in the percent of fractional shortening (%FS), a parameter for contractile function, as early as 1 week after tamoxifen treatment in PDK1-MerCre mice (Fig. 1 *C* and *D*). During this period, there was no increase in LV dimension or thinning of LV wall, which was consistent with the macroscopic findings (Fig. 1 *B* and *D*). However, 4 weeks after tamoxifen treatment, progression of contractile dysfunction together with global chamber dilatation and wall thinning was observed in PDK1-MerCre mice (Fig. 1 *B* and *E*). Histologically, interstitial fibrosis was increased at 1 week in

PDK1-MerCre hearts and further enhanced at 4 weeks after tamoxifen treatment (Fig. 1*F*). These results suggest that PDK1-MerCre mice exhibited cardiac dysfunction as early as 1 week after tamoxifen treatment and LV remodeling at 4 weeks.

It was reported that PDK1-MCKCre showed marked reduction both in the heart size and in cardiac contractility (5). Since the *MCK* promoter directs expression of Cre recombinase before birth (5, 12), retardation of heart growth that was not proportional to somatic growth after birth might lead to cardiac dysfunction. However, the surface areas of caridomyocytes were not significantly different between PDK1-MerCre mice and control mice 1 week after tamoxifen treatment (Fig. 1*G*). Given that LV dysfunction was already observed as early as 1 week after tamoxifen treatment (Fig. 1 *C* and *D*), we suppose that reduction of cardiomyocyte size is not critically involved in the impairment of LV contraction observed in PDK1-MerCre hearts.

**Increased Cardiomyocyte Apoptosis in PDK1-MerCre Mice.** We next examined whether cardiomyocyte apoptosis was involved in the pathogenesis of heart failure in PDK1-MerCre mice. TUNEL staining revealed that the number of apoptotic cells was dramatically increased in PDK1-MerCre hearts 1 week after tamoxifen treatment (Fig. 2*A*). TUNEL-positive cells were cardiomyocytes, because these cells were positively stained with anti-sarcomeric α-actinin antibody (Fig. 2*B*). In addition, immunostaining revealed an increase in cardiomyocytes positively stained for cleaved caspase-3 in PDK1-MerCre hearts (Fig. 2*C*). The prevalence of TUNEL-positive cardiomyocytes was 1.14 ± 0.05% of total cardiomyocytes (Fig. 2*D*). Therefore, cardiomyocyte loss through apoptotic cell death may play an important role in the pathogenesis of heart failure in PDK1-MerCre mice.

In the hearts of PDK1-MerCre, the expression level of proapoptotic Bax was increased, whereas those of anti-apoptotic molecules such as Bcl-2 and Bcl-xL were unchanged (Fig. 2*E*). SGK1 has been reported to be functionally anti-apoptotic in the hearts (13). The basal level of phosphorylated SGK1 was reduced in PDK1-MerCre hearts (Fig. 2*F*). It has been reported that SGK1, in concert with Akt, mediates cell survival by phosphorylating and inactivating the Forkhead transcription factor FOXO3a (13, 14). FOXO3a is phosphorylated at Thr-32 and Ser-315 by SGK1, and Akt favors the phosphorylation of Thr-32 and Ser-253 (14). In PDK1-MerCre hearts, phosphorylation levels of FOXO3a at Thr-32 and Ser-253 were significantly decreased (Fig. 2*F*). Collectively, these results suggest that up-regulation of Bax protein and reduction of Akt and SGK1 activity were potentially involved in enhancing susceptibility of cardiomyocytes to apoptosis in PDK1-MerCre mice.

**Overexpression of Bcl-2 Protein Prevented Cardiomyocyte Apoptosis and Partially Rescued Cardiac Dysfunction in PDK1-MerCre Mice.** To examine whether cardiomyocyte apoptosis plays a causative role in the pathogenesis of heart failure in PDK1-MerCre mice, we crossed PDK1-MerCre with transgenic mice with cardiac-specific overexpression of Bcl-2 (Bcl2-Tg mice) (15). In PDK1-MerCre × Bcl2-Tg hearts, the number of TUNEL-positive cardiomyocytes was significantly decreased in comparison with PDK1-MerCre hearts (Fig. 2*G*), and the %FS showed partial but significant improvement (Fig. 2*H*). These results suggest that cardiac dysfunction is caused in part by cardiomyocyte loss through apoptosis in PDK1-MerCre mice.

**Impairment of β-adrenergic Responsiveness in PDK1-MerCre Hearts.** Incomplete restoration of cardiac function by prevention of cardiomyocyte apoptosis implies that some functional abnormalities persist in viable cardiomyocytes in PDK1-MerCre mice. To determine whether β-adrenergic responsiveness was changed in PDK1-MerCre hearts, we carried out Langendorff perfusion analysis in the hearts 1 week after tamoxifen treatment, and evaluated responsiveness to isoproterenol, a β-AR agonist, and forskolin, an activator of adenylate cyclase that increases cAMP independently

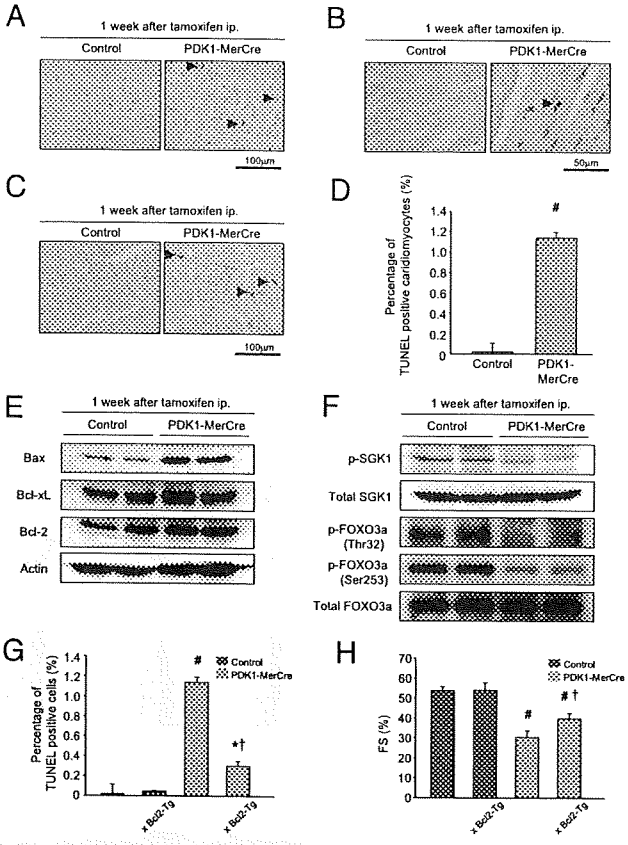


**Fig. 2.** Cardiomyocyte apoptosis in the pathogenesis of heart failure in PDK1-MerCre mice. (*A*) TUNEL staining. Arrowheads indicate TUNEL-positive cardiomyocytes. (*B*) Double staining for TUNEL staining (brown) and sarcomeric α-actinin (red). Arrowheads indicate TUNEL-positive cardiomyocytes. (*C*) Immunostaining for cleaved caspase-3. Arrowheads indicate cardiomyocytes positively stained for cleaved caspase-3. (*D*) Percentage of TUNEL-positive caridomyocytes. Values represent the mean ± SEM (3,000 cardiomyocytes in each group). #, $P < 0.01$ versus control group. (*E*) Immunoblot analysis of Bcl-2 family proteins in the hearts. (*F*) Immunoblot analysis of phosphorylated-SGK1 at Ser-78, total SGK1, phosphorylated-FOXO3a at Thr-32 or at Ser-253, and total FOXO3a in the hearts. (*G*) Percentage of TUNEL-positive caridomyocytes in control, Bcl2-Tg, PDK1-MerCre, and PDK1-MerCre × Bcl2-Tg mice. Values represent the mean ± SEM (3,000 cardiomyocytes in each group). #, $P < 0.01$ versus control group; *, $P < 0.05$, versus control group; †, $P < 0.01$ versus PDK1-MerCre group. (*H*) Measurement of fractional shortening of control, Bcl2-Tg, PDK1-MerCre, and PDK1-MerCre × Bcl2-Tg mice by echocardiography. Values represent the mean ± SEM of data from control mice (n = 10), control × Bcl2-Tg mice (n = 6), PDK1-MerCre mice (n = 10), and PDK1-MerCre × Bcl2-Tg mice (n = 6). #, $P < 0.01$ versus control mice. †, $P < 0.01$ versus PDK1-MerCre mice. FS, % of fractional shortening.

of β-AR. As shown in Fig. 3*A*, the baseline parameters of +dp/dt and −dp/dt were significantly lower in PDK1-MerCre mice than in control mice. Both isoproterenol and forskolin induced positive chronotropic and inotropic responses in control mice (Fig. 3*A*). However, PDK1-MerCre mice showed a significant reduction in the maximal changes in HR, +dP/dt, and −dP/dt after the stimulation of isoproterenol ($1 \times 10^{-8}$ M), compared with control mice (Fig. 3*B*). In contrast, the maximal changes in these parameters after the stimulation of forskolin ($1 \times 10^{-7}$ M) did not differ significantly between PDK1-MerCre and control mice (Fig. 3*B*). These results suggest that the responsiveness of β-AR is impaired in PDK1-MerCre mice.

Next, we measured the amount of $\beta_1$-AR in the membrane fraction by immunoblot analysis. In PDK1-MerCre hearts, the expression levels of $\beta_1$-AR in membrane fraction were markedly

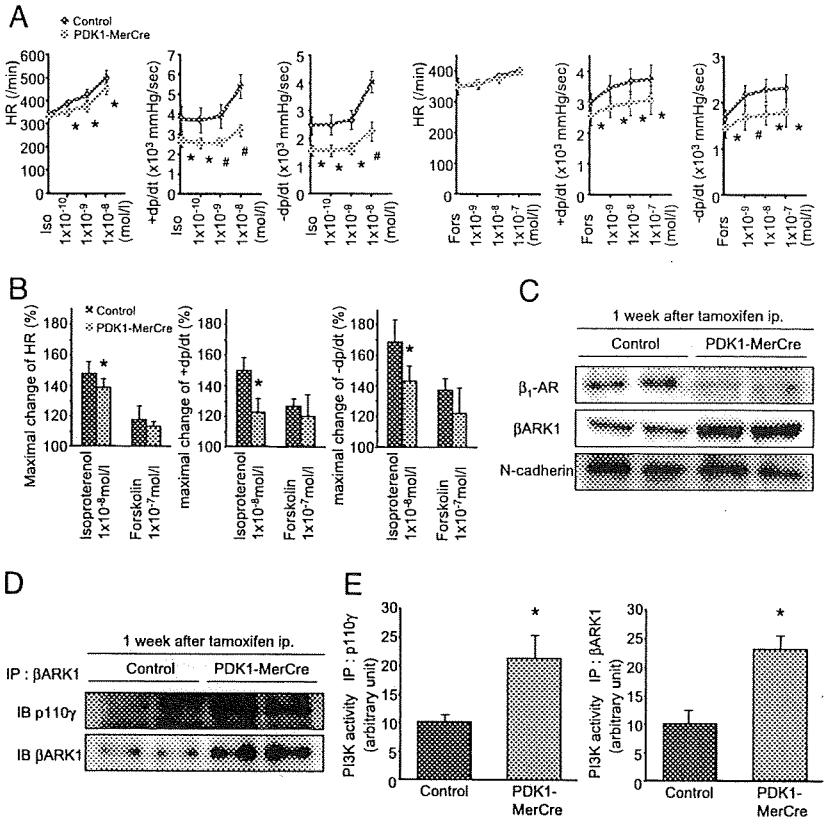


**Fig. 3.** Impaired β-adrenergic responsiveness in PDK1-MerCre mice. (*A*) Effects of isoproterenol and forskolin on heart rate, contraction, and relaxation in Langendorff-perfused mouse hearts 1 week after tamoxifen treatment. +dp/dt, maximum rate of LV pressure development; −dp/dt, maximum rate of LV pressure decline; HR, heart rate. Values represent the mean ± SEM. *, $P < 0.05$ versus control group, #, $P < 0.01$ versus control group. (*B*) The % changes in HR, +dP/dt, and −dP/dt before and after treatment with isoproterenol ($1 \times 10^{-8}$ M) or forskolin- ($1 \times 10^{-7}$ M) were calculated. Values represent the mean ± SEM. *, $P < 0.05$ versus control group. (*C*) Immunoblot analysis of $\beta_1$-AR and βARK1 in membrane fraction of the hearts. N-cadherin was used as an internal control for the amount of membrane protein. (*D*) Immunoblot analysis of βARK1-associated p110γ protein in the hearts. (*E*) Kinase assays for PI3-K activity. The hearts were subjected to immunoprecipitaion with antibody to p110γ, or βARK1, and the resulting precipitates were assayed for the kinase assay. PI3-K activity of control mice was adjusted to 10 arbitrary units.

down-regulated (Fig. 3*C*). Inversely, the amount of $\beta_1$-AR in cytosolic fraction was increased in PDK1-MerCre hearts, compared with control hearts, while the total amount of $\beta_1$-AR was unchanged (Fig. S3 *A* and *B*), suggesting that receptor internalization underlies $\beta_1$-AR down-regulation in membrane fraction of PDK1-MerCre hearts. In response to β-AR simulation, increased cAMP activates protein kinase A (PKA), which directly phosphorylates phospholamban (PLN) at Ser-16. PDK1-MerCre hearts showed a significant decrease in cAMP concentrations (Fig. S3*C*) and phosphorylation level of PLN at Ser-16 (Fig. S3*D*), compared with control hearts. Phosphorylated PLN dissociates from sarcoplasmic reticulum $Ca^{2+}$-ATPase2 (SERCA2) and thereby enhances $Ca^{2+}$ uptake by SERCA2, which leads to enhancement of cardiac contractility (2). These results suggest that, in PDK1-MerCre hearts, robust $\beta_1$-AR internalization leads to contractile dysfunction.

It has been reported that phosphorylation of β-AR by β-AR kinase 1 (βARK1, commonly known as G protein-coupled receptor kinase 2) regulates receptor internalization (16). In the hearts of PDK1-MerCre mice 1 week after tamoxifen treatment, the expression levels of βARK1 (Fig. 3*C*) and βARK1-associated p110γ, a catalytic subunit of PI3-Kγ, were increased (Fig. 3*D*). Notably, PI3-K activity immunoprecipitated with antibodies to either p110γ or βARK1 was enhanced (Fig. 3*E*) in PDK1-MerCre hearts. βARK1 forms complex with PI3-Kγ through the phosphoinositide kinase (PIK) domain, and protein kinase activity of PI3-Kγ in this complex is required for receptor internalization (17). Therefore, these results suggest that enhanced PI3-Kγ activity in PDK1-MerCre hearts increases βARK1/PI3-Kγ complex formation, and that βARK1 phosphorylates β-AR to cause robust receptor internalization.

**Disruption of βARK1/PI3-Kγ Complex Restored β-AR Internalization and Partially Rescued Cardiac Dysfunction in PDK1-MerCre Mice.** To corroborate that enhanced PI3-Kγ activity promotes β-AR internalization by forming complex with βARK1 and that robust β-AR internalization causes cardiac dysfunction, we examined whether disruption of the βARK1/PI3-Kγ complex normalizes β-AR trafficking and improves cardiac function in PDK1-MerCre mice. For that purpose, we crossed PDK1-MerCre mice with transgenic mice harboring cardiac-specific overexpression of PIK domain (PIK-Tg mice) (16), which competitively inhibits the association between βARK1 and PI3-Kγ. The amount of βARK1-associated p110γ protein was significantly decreased in PDK1-MerCre × PIK-Tg mice, compared with PDK1-MerCre mice (Fig. 4*A*). Importantly, βARK1-associated PI3-K activity was markedly decreased in PDK1-MerCre × PIK-Tg mice, compared with PDK1-MerCre mice (Fig. 4*B*, *Lower*), although total PI3-Kγ activity remained elevated (Fig. 4*B*, *Upper*). As a consequence, in PDK1-MerCre × PIK-Tg mice 1week after tamoxifen treatment, the expression levels of $\beta_1$-AR in membrane fraction were restored (Fig. 4*C*). The %FS in echocardiographic examination showed partial but significant improvement (Fig. 4*D*). Overexpression of PIK domain did not influence cardiomyocyte apoptosis, because the prevalence of TUNEL-positive cardiomyocytes (Fig. 4*E*), as well as the amount of cleaved poly(ADP-ribose) polymerase, Bax, and phosphrylated FOXO3a (Fig. S4), was unchanged in PDK1-MerCre hearts. In addition, overexpression of Bcl-2 protein did not influence β-adrenergic response, because the amount of βARK1-associated p110γ protein (Fig. 4*A*), βARK1-associated PI3-K activity (Fig. 4*B*), the expression levels of membranous $\beta_1$-AR (Fig. 4*C*), as well as cAMP concentration and phosphorylation levels of PLN at Ser-16 (Fig. S5), were unchanged in PDK1-MerCre hearts. These results suggest that enhancement of βARK1-associated PI3-Kγ activity induces robust β-AR internalization, and thereby contributes to cardiac dysfunction, independently of cardiomyocyte apoptosis, in PDK1-MerCre mice.

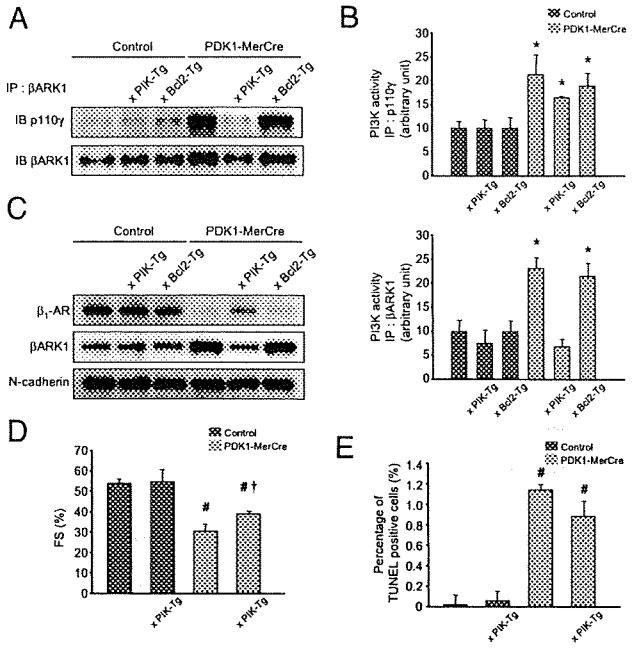


**Fig. 4.** Alleviated cardiac dysfunction in PDK1-MerCre mice by overexpression of PIK domain or Bcl-2 protein. (*A*) Immunoblot analysis of βARK1-associated p110γ protein in the hearts. (*B*) Kinase assays for PI3-K activity in the hearts. The hearts were subjected to immunoprecipitaion with antibody to p110γ (*Upper*) or βARK1 (*Lower*), and the resulting precipitates were assayed for the kinase assay. PI3-K activity of control mice was adjusted to 10 arbitrary units. (*C*) Immunoblot analysis of $\beta_1$-AR and βARK1 in membrane fraction in the hearts. N-cadherin was used as an internal control for the amount of membrane protein. (*D*) Fractional shortening measured by echocardiography. Values represent the mean ± SEM of data from control mice (n = 10), control × PIK-Tg mice (n = 6), PDK1-MerCre mice (n = 10), and PDK1-MerCre × PIK-Tg mice (n = 6). #, $P < 0.01$ versus control mice. †, $P < 0.01$ versus PDK1-MerCre mice. FS, % of fractional shortening. (*E*) Percentage of TUNEL-positive cardiomyocytes. Values represent the mean ± SEM (3,000 cardiomyocytes in each group). #, $P < 0.01$ versus control group. †, $P < 0.01$ versus PDK1-MerCre group.

## Discussion

Our present study revealed that PDK1 plays an integrative role in normal cardiac function by coordinating survival signals and β-adrenergic response (Fig. S6). Besides the fundamental role in promoting cell growth and survival observed in many tissues in common (18–21), PDK1 uniquely accommodates β-adrenergic response to prevent cardiac decompensation. In addition, decreased expression of PDK1 protein in experimental models of heart failure raises a possibility that functional alterations of PDK1 may be implicated in the pathogenesis of heart failure, although it remains unclear how PDK1 expression is regulated in stressed hearts.

β-AR signaling plays a pivotal role in the chronotropic and inotropic functions in the hearts (22). In PDK1-MerCre hearts, the activity of βARK1-associated PI3-Kγ was enhanced, which enforced robust $\beta_1$-AR down-regulation. PDK1 is a direct downstream effector of PI3-K and may participate in the negative feedback regulation of PI3-K signaling pathway (20). Importantly, overexpression of PIK-domain prevented $\beta_1$-AR down-regulation by interfering βARK1/PI3-Kγ complex formation, and alleviated cardiac dysfunction in PDK1-MerCre mice. A recent report demonstrated that PI3-Kγ negatively modulates cardiac contractility by promoting phosphodiesterase 3B-mediated destruction of cAMP in a kinase-independent manner (23), but we did not observe significant change in the activity of phosphodiesterase 3B in PDK1-MerCre hearts despite enhanced PI3-Kγ activity (Fig. S7). Therefore, we suppose that impairment of β-adrenergic responsiveness results from intense β-AR down-regulation in PDK1-MerCre hearts.

It remains controversial whether down-regulation and desensitization of β-AR function is beneficial or detrimental in failing hearts. Indeed, clinical trials have indicated that the use of β-AR antagonists improves morbidity and mortality in patients of heart failure (1). Sustained β-AR overstimulation promotes energy consumption and apoptosis in cardiomyocytes (1, 24). But, accumulating evidence has suggested that normalization of β-adrenergic signaling by interfering βARK1 function rescued numerous genetic and experimental models of heart failure in mice (16, 25–28). A possible explanation for this discrepancy is that the therapeutic window for optimal level of β-AR signaling may be narrow in failing hearts (22, 28). It has been reported that the proapoptotic effect of $\beta_1$-AR stimulation is dependent on $Ca^{2+}$/calmodulin-dependent kinase II (CaMKII) (24). The phosphorylation level of CaMKII was decreased in PDK1-MerCre hearts, and restored to a subnormal level by overexpression of PIK domain (Fig. S8). Importantly, normalization of $\beta_1$-AR did not induce excessive activation of CaMKII and cardiomyocyte apoptosis (Fig. 4*E* and Fig. S4). Thus, the $\beta_1$-AR normalization may improve contractile function without evoking a 'fight or flight' reaction, unlike the simple $\beta_1$-AR activation. Alternatively, robust β-AR internalization may activate adverse intracellular signaling pathways through β-arrestins (29) and abrogate the cardioprotective effects mediated by transactivation of epidermal growth factor receptor (30). Further investigations will be required to clarify the entire mechanisms of how normalization of β-AR signaling confers therapeutic benefits on failing hearts.

A growing body of evidence has suggested that cardiomyocyte apoptosis plays an important role in the pathogenesis of heart failure (31). In PDK1-MerCre hearts, the phosphorylation levels of Akt, SGK1 and FOXO3a were reduced, which may give rise to marked increase in cardiomyocyte apoptosis. In addition, PDK1-MerCre hearts showed an increase in expression level of Bax protein, a key molecule that translocates to the mitochondrial membrane and triggers the release of cytochrome *c* into the cytoplasm (31). Overexpression of Bcl-2 attenuated apoptotic loss of cardiomyocytes and alleviated cardiac dysfunction in PDK1-MerCre mice, suggesting that cardiomyocyte apoptosis contributes to the development of heart failure.

The previous paper demonstrated that PDK1-MCKCre mice showed growth retardation and contractile dysfunction of cardimyocytes (5). In our study, PDK1-MerCre mice showed severe heart failure without alterations in cardiomyocyte size. Besides regulation of cell growth, PDK1 controls cardiac homeostasis by promoting cell survival and preserving β-AR response. The phenotypic difference between PDK1-MerCre mice and PDK1-MCKCre mice resulted from the timing of gene disruption. The *Pdk1* gene was deleted within a week in tamoxifen-treated PDK1-MerCre hearts of adult mice, but in contrast, *Pdk1* disruption commenced before birth in PDK1-MCKCre mice. The number of apoptotic cardiomyocytes was pronouncedly increased in PDK1-MerCre hearts, but was unchanged in PDK1-MCKCre hearts (5). Some compensation mechanisms may prevent proapoptotic effects of *Pdk1* disruption in PDK1-MCKCre mice.

In conclusion, PDK1 is a pivotal effector with dual functions to promote survival of cardiomyocytes and to preserve β-AR response in vivo (Fig. S6). In this regard, up-regulation of PDK1 in the hearts may emerge as a potential therapeutic strategy for heart failure.

## Methods

**Generation of PDK1-MerCre Mice.** Mice harboring a *Pdk1*$^{flox}$ allele were previously described (7, 8). Mice expressing MerCreMer under the control of *α-myosin heavy chain* promoter were previously described (9). Details are in *SI Methods*. Bcl2-Tg mice and PIK-Tg mice were kindly gifted by Dr. Michael D. Schneider (Imperial

College, London, U.K.) (15) and Dr. Howard A. Rockman (Duke University Medical Center, Durham, NC) (16). All of the experimental protocols were approved by the Institutional Animal Care and Use Committee of Chiba University.

**Echocardiography and Isolated Heart Preparation.** Transthoracic echocardiography was performed on conscious mice with Vevo 660 Imaging System using a 25-MHz linear probe (Visual Sonics Inc.). For analyses of hemodynamic parameters, hearts were excised rapidly and mounted on a Langendorff perfusion system, and a balloon was inserted into the cavity of the left ventricle (32). Isolated hearts were stabilized for 30 min by perfusion of Krebs-Henseleit buffer followed by perfusion of isoproterenol (NIKKEN Chemical Laboratory) or forskolin (Sigma). For measurement of surface areas of cardiomyocytes, hearts were enzymatically dissociated as described previously (33).

**Histological Analysis and Immunohistochemistry.** Hearts were excised and immediately fixed in 10% neutralized formalin, embedded in paraffin. Serial sections at 5 $\mu$m were stained with hematoxylin and eosin for morphological analysis, and with Masson's trichrome for detection of fibrosis. For immunohistochemistry, Vectastain ABC kit (Vector Laboratories) was used to detect the primary antibodies. TUNEL assay was performed on paraffin sections, using an in situ apoptosis detection kit (Takara Bio Inc.).

**Western Blot Analysis and Subcellular Fractionation.** Protein samples were fractionated by SDS/PAGE, and immunoblot analysis was performed as described previously (34). The membrane and cytosol fractions were isolated from lysate of the hearts as previously described (35).

**Assay for PI3-K Activities.** PI3-K acitivity was measured as previously described (36). We determined Akt activity using a Akt Kinase Assay Kit according to the manufacturer's protocol (Cell Signaling Technology).

**Antibodies.** The following antibodies were used: p110$\gamma$, phosphorylated-SGK, and cleaved caspase-3 (Cell Signaling Technology), $\beta$ARK1, Bax, Bcl-xL, Bcl-2 (Santa Cruz Biotechnology), $\beta_1$-AR (Affinity BioReagents), N-cadherin (Zymed Laboratories Inc.), SGK1, FOXO3a, phosphorylated-FOXO3a (Thr-32), phosphorylated-FOXO3a (Ser-253) (Upstate) and actin (Sigma).

**Statistical Analysis.** All data are presented as means ± SEM. All data were analyzed by one-way ANOVA followed by the Fisher procedure for comparison of means. A probability value of $P < 0.05$ was considered to be statistically significant.

**ACKNOWLEDGMENTS.** We thank Drs. M. D. Schneider and H. A. Rockman for generously providing Bcl2-Tg and PIK-Tg mice, respectively. We thank M. Akao and Y. Oike for technical advice, and A. Furuyama, M. Ikeda, Y. Ohtsuki, and I. Sakamoto for their excellent technical assistance. This work was supported in part by grants from the Japanese Ministry of Education, Science, Sports, and Culture, and Health and Labor Sciences Research Grants (to IK and HA); grants from Japan Intractable Diseases Research Foundation, Kowa Life Science Foundation, and Takeda Science Foundation (to HA).

1. Katz AM (2008) The "modern" view of heart failure: How did we get here?. *Circ Heart Fail* 1:63–71.
2. Mudd JO, Kass DA (2008) Tackling heart failure in the twenty-first century. *Nature* 451:919–928.
3. Toker A, Newton AC (2000) Cellular signaling: Pivoting around PDK-1. *Cell* 103:185–188.
4. Lawlor MA, et al. (2002) Essential role of PDK1 in regulating cell size and development in mice. *EMBO J* 21:3728–3738.
5. Mora A, et al. (2003) Deficiency of PDK1 in cardiac muscle results in heart failure and increased sensitivity to hypoxia. *EMBO J* 22:4666–4676.
6. Budas GR, Sukhodub A, Alessi DR, Jovanovic A (2006) 3'Phosphoinositide-dependent kinase-1 is essential for ischemic preconditioning of the myocardium. *FASEB J* 20:2556–2558.
7. Sakaue H, et al. (2003) Requirement for 3-phosphoinositide-kependent dinase-1 (PDK-1) in insulin-induced glucose uptake in immortalized brown adipocytes. *J Biol Chem* 278:38870–38874.
8. Inoue H, et al. (2006) Role of hepatic STAT3 in brain-insulin action on hepatic glucose production. *Cell Metab* 3:267–275.
9. Sohal DS, et al. (2001) Temporally regulated and tissue-specific gene manipulations in the adult and embryonic heart using a tamoxifen-inducible Cre protein. *Circ Res* 89:20–25.
10. Williams MR, et al. (2000) The role of 3-phosphoinositide-dependent protein kinase 1 in activating AGC kinases defined in embryonic stem cells. *Curr Biol* 10:439–448.
11. Manning BD, Cantley LC (2007) AKT/PKB signaling: Navigating downstream. *Cell* 129:1261–1274.
12. Bruning JC, et al. (1998) A muscle-specific insulin receptor knockout exhibits features of the metabolic syndrome of NIDDM without altering glucose tolerance. *Mol Cell* 2:559–569.
13. Aoyama T, et al. (2005) Serum and glucocorticoid-responsive kinase-1 regulates cardiomyocyte survival and hypertrophic response. *Circulation* 111:1652–1659.
14. Brunet A, et al. (2001) Protein kinase SGK mediates survival signals by phosphorylating the forkhead transcription factor FKHRL1 (FOXO3a). *Mol Cell Biol* 21:952–965.
15. Imahashi K, Schneider MD, Steenbergen C, Murphy E (2004) Transgenic expression of Bcl-2 modulates energy metabolism, prevents cytosolic acidification during ischemia, and reduces ischemia/reperfusion injury. *Circ Res* 95:734–741.
16. Perrino C, et al. (2005) Restoration of beta-adrenergic receptor signaling and contractile function in heart failure by disruption of the betaARK1/phosphoinositide 3-kinase complex. *Circulation* 111:2579–2587.
17. Naga Prasad SV, Jayatilleke A, Madamanchi A, Rockman HA (2005) Protein kinase activity of phosphoinositide 3-kinase regulates beta-adrenergic receptor endocytosis. *Nat Cell Biol* 7:785–796.
18. Mora A, Lipina C, Tronche F, Sutherland C, Alessi DR (2005) Deficiency of PDK1 in liver results in glucose intolerance, impairment of insulin-regulated gene expression and liver failure. *Biochem J* 385:639–648.
19. Hashimoto N, et al. (2006) Ablation of PDK1 in pancreatic beta cells induces diabetes as a result of loss of beta cell mass. *Nat Genet* 38:589–593.
20. Okamoto Y, et al. (2007) Restoration of glucokinase expression in the liver normalizes postprandial glucose disposal in mice with hepatic deficiency of PDK1. *Diabetes* 56:1000–1009.
21. Belgardt BF, et al. (2008) PDK1 deficiency in POMC-expressing cells reveals FOXO1-dependent and -independent pathways in control of energy homeostasis and stress response. *Cell Metab* 7:291–301.
22. Rockman HA, Koch WJ, Lefkowitz RJ (2002) Seven-transmembrane-spanning receptors and heart function. *Nature* 415:206–212.
23. Patrucco E, et al. (2004) PI3Kgamma modulates the cardiac response to chronic pressure overload by distinct kinase-dependent and -independent effects. *Cell* 118:375–387.
24. Zhu WZ, et al. (2003) Linkage of beta1-adrenergic stimulation to apoptotic heart cell death through protein kinase A-independent activation of Ca2+/calmodulin kinase II. *J Clin Invest* 111:617–625.
25. Harding VB, Jones LR, Lefkowitz RJ, Koch WJ, Rockman HA (2001) Cardiac beta ARK1 inhibition prolongs survival and augments beta blocker therapy in a mouse model of severe heart failure. *Proc Natl Acad Sci USA* 98:5809–5814.
26. Shah AS, et al. (2001) In vivo ventricular gene delivery of a beta-adrenergic receptor kinase inhibitor to the failing heart reverses cardiac dysfunction. *Circulation* 103:1311–1316.
27. Nienaber JJ, et al. (2003) Inhibition of receptor-localized PI3K preserves cardiac beta-adrenergic receptor function and ameliorates pressure overload heart failure. *J Clin Invest* 112:1067–1079.
28. Raake PW, et al. (2008) G protein-coupled receptor kinase 2 ablation in cardiac myocytes before or after myocardial infarction prevents heart failure. *Circ Res* 103:413–422.
29. Lefkowitz RJ, Shenoy SK (2005) Transduction of receptor signals by beta-arrestins. *Science* 308:512–517.
30. Noma T, et al. (2007) Beta-arrestin-mediated beta1-adrenergic receptor transactivation of the EGFR confers cardioprotection. *J Clin Invest* 117:2445–2458.
31. Foo RS, Mani K, Kitsis RN (2005) Death begets failure in the heart. *J Clin Invest* 115:565–571.
32. Suzuki M, et al. (2001) Functional roles of cardiac and vascular ATP-sensitive potassium channels clarified by Kir6.2-knockout mice. *Circ Res* 88:570–577.
33. Sambrano GR, et al. (2002) Navigating the signalling network in mouse cardiac myocytes. *Nature* 420:712–714.
34. Akazawa H, et al. (2004) Diphtheria toxin-induced autophagic cardiomyocyte death plays a pathogenic role in mouse model of heart failure. *J Biol Chem* 279:41095–41103.
35. Takeishi Y, Jalili T, Ball NA, Walsh RA (1999) Responses of cardiac protein kinase C isoforms to distinct pathological stimuli are differentially regulated. *Circ Res* 85:264–271.
36. Sakaue H, et al. (1997) Phosphoinositide 3-kinase is required for insulin-induced but not for growth hormone- or hyperosmolarity-induced glucose uptake in 3T3-L1 adipocytes. *Mol Endocrinol* 11:1552–1562.

# Impact of QT Variables on Clinical Outcome of Genotyped Hypertrophic Cardiomyopathy

Katsuharu Uchiyama, M.D., Kenshi Hayashi, M.D., Noboru Fujino, M.D., Tetsuo Konno, M.D., Yuichiro Sakamoto, M.D., Kenji Sakata, M.D., Masa-aki Kawashiri, M.D., Hidekazu Ino, M.D., and Masakazu Yamagishi, M.D.

*From the Division of Cardiovascular Medicine, Kanazawa University Graduate School of Medicine, Kanazawa, Japan*

**Background:** Although QT variables such as its interval and/or dispersion can be clinical markers of ventricular tachyarrhythmia, few data exist regarding the role of QT variables in genotyped hypertrophic cardiomyopathy (HCM). Therefore, we analyzed QT variables in genotyped subjects with or without left ventricular hypertrophy (LVH).

**Methods:** QT variables were analyzed in 111 mutation and 43 non-mutation carriers who were divided into three groups: A, those without ECG abnormalities and echocardiographically determined LVH (wall thickness ≥13 mm); B, those with ECG abnormalities but LVH; and C, those with ECG abnormalities and LVH. We also examined clinical outcome of enrolled patients.

**Results:** Maximal LV wall thickness in group C (19.0 ± 4.3 mm, mean ±SD) was significantly greater than that in group A (9.2 ± 1.8) and group B (10.4 ± 1.8). Under these conditions, maximum QTc interval and QT dispersion were significantly longer in group C than those in group A (438 ± 38 ms vs 406 ± 30 and 64 ± 31 vs 44 ± 18, respectively; $P < 0.05$). QTc interval and QT dispersion in group B (436 ± 50 and 64 ± 22 ms) were also significantly greater than those in group A. During follow-up periods, four sudden cardiac deaths and one ventricular fibrillation were observed in group C, and two nonlethal ventricular tachyarrhythmias were observed in group B.

**Conclusions:** Patients with HCM-related gene mutation accompanying any ECG abnormalities frequently exhibited impaired QT variables even without LVH. We suggest that careful observation should be considered for those genotyped subjects.

**Ann Noninvasive Electrocardiol 2009;14(1):65–71**

hypertrophic cardiomyopathy; QT dispersion; gene mutation

Hypertrophic cardiomyopathy (HCM) is an inherited cardiac disease that is caused by mutation of the genes, encoding sarcomeric proteins.[1] Patients with HCM are known as high risk of sudden cardiac death and/or malignant ventricular tachyarrhythmia (SCD/VT).[2] Importantly, SCD may be the first clinical manifestation.[3]

QT variables such as QT intervals and QT dispersion were evaluated in patients with HCM, and QT dispersion[4,5] and T-peak to T-end interval[6] were reported as markers for SCD/VT in such patients. However, few data existed regarding relationship between the presence and absence of left ventricular hypertrophy (LVH) and those of QT variables, because the causes of LVH were complicated for analysis.

Advances in molecular genetics enable us showing whether individuals in HCM families have a gene mutation.[7–9] Consequently, the appearance of abnormal QT variables can be examined in genotyped subjects with or without LVH. The aim of this study was to examine relationship between LVH and abnormal QT variables in genotyped subjects and to examine impact of abnormal QT variables on clinical outcome in these subjects.

## METHODS

### Study Population

The study population consisted of 111 genotyped subjects from kindred with HCM associated

*Address for reprints: Masakazu Yamagishi, M.D., Division of Cardiovascular Medicine, Kanazawa University Graduate School of Medicine, Takara-Machi 13-1, Kanazawa 920-8640, Japan. Fax: +81-76-234-4251; E-mail: myamagi@med.kanazawa-u.ac.jp*

with the beta-myosin heavy-chain gene mutations (Ala26Val, Ala200Thr, Met822Leu, Arg858Cys, Ser866Pro, Arg870Cys, Glu935Lys), the myosin-binding protein-C gene mutations (c.2067 + 1G→A, c.1777delT, Arg820Gln), the cardiac troponin T gene mutations (Val85Leu, Arg92Trp, Phe110Ile, Lys273Glu), or the cardiac troponin I gene mutation (Lys183del) identified in Kanazawa University Hospital. All mutations except Ala200Thr, Met822Leu, Arg858Cys, and Ser866Pro have been previously identified and described elsewhere.[7,8,10–15] Informed consent was obtained from all participants or from their guardians, in accordance with the guidelines of the Bioethical Committee on Medical Research, Kanazawa University Graduate School of Medicine. Subjects with a clinical cause of LVH such as hypertension or severe valvular heart disease were excluded from this analysis.

Groups were classified as follows: mutation carriers without any ECG abnormalities and LVH (group A), carriers with ECG abnormalities but without LVH (group B), and carriers with ECG abnormalities and LVH (group C). As controls, 43 unaffected subjects from the same kindred were selected and divided into two groups, because there were age differences between groups A and B.

## Electrocardiographic Examinations

Standard 12-lead ECG was recorded in all subjects at paper speed of 25 mm/s with a gain of 10 mm/mV. All records were magnified by 200% and QT intervals were manually measured. In order to eliminate both interobserver variability and bias, QT intervals were measured using a digitizer in each of the 12 leads by a single observer who was blinded to all clinical findings. The QT interval was measured from the onset of the QRS complex to the end of the T wave at $V_5$ lead. The end of the T wave was defined as the intersecting point of a tangent line on the terminal T wave and the TP baseline.[6] When a U wave was present, QT was measured to the nadir of the curve between the T and U waves. QT intervals were corrected for heart rate using Bazett's formula such as $QTc = QT/RR^{1/2}$.

QT dispersion was calculated as the difference between the maximum QT and minimum QT intervals on all 12 leads of the ECG. If the height or depth of the T wave was <1.5 mm, this lead was excluded from the analysis.[16] T-peak to T-end interval, which represents transmural dispersion of repolarization,[17] was also measured as the interval between the peak and end of T wave at $V_5$ lead.

In addition to QT analysis, we also defined ECG abnormalities as follows: (1) Q wave >0.04 second in duration or more than one fourth of the ensuring R wave in depth in at least two leads except in aVR[18]; (2) LVH assessed by a Romhilt-Estes score >4[19,20]; (3) ST-segment depression of an upsloping type >0.1 mV at 0.08 second after the J point, or those of horizontal or downsloping type >0.05 mV; and (4) T-wave inversion >0.1 mV except in aVR and $V_1$ to $V_2$ leads in the absence of conduction disturbance.[21]

## Echocardiographic Examinations

Standard transthoracic M-mode and two-dimensional echocardiographic studies were performed to identify and quantify morphologic features of the left ventricle. Left ventricular dimensions and the thicknesses of the septum and posterior wall were measured at the level of the tips of the mitral valve leaflet. Wall hypertrophy was defined as maximum left ventricular wall thickness ≥13 mm in adults or >95% CI of the theoretical value in children.[22] Additionally, we measured anterior and lateral walls of LV at the same level of measuring septum and posterior wall. From these measurements, we defined the maximal LV wall thickness (Fig. 1).

## Survival Analysis

Data on survival and clinical status were collected at the time of visit of patients and were followed at this hospital and by direct telephone interview with patients, their family members, or their attending physicians at affiliated hospitals. The end points were defined as aborted cardiac arrest and SCD. Minor cardiac event such as nonlethal arrhythmia was also recorded. Enhanced antiarrhythmic treatments such as implantable cardioverter defibrillator (ICD) and amiodarone were not used until lethal arrhythmia occurred.

## Statistical Analysis

Values are expressed as the mean ±SD. Comparison between the groups was performed using a one-way analysis of variance (ANOVA) followed by Scheffe's method. Categorical data were compared using chi-square analysis. Analysis was

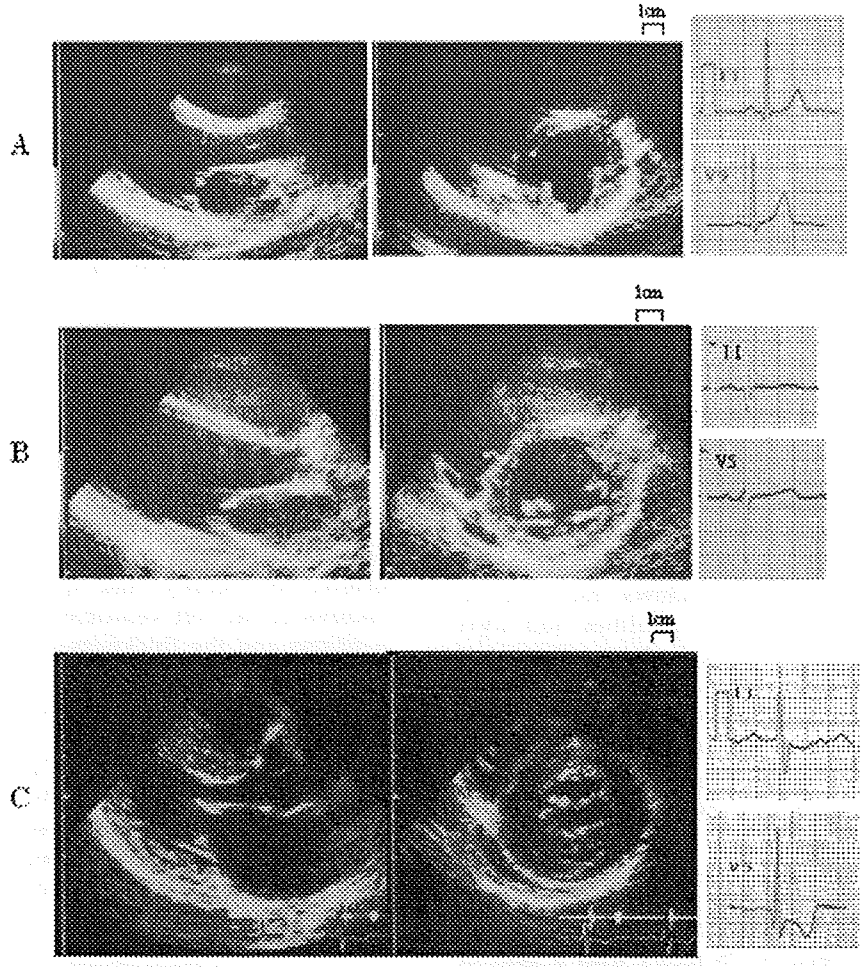


**Figure 1.** Representative cases for examination. (A) A case with neither ECG abnormalities nor LVH (group A). (B) A case with ECG abnormalities such as deep Q wave without LVH (group B). (C) A case both with ECG abnormalities such as abnormal Q waves and negative T waves and LVH (group C).

performed using StatView 5.0 (Abacus Concepts, Inc., Berkeley, CA, USA). A P value $<0.05$ was considered statistically significant.

## RESULTS

### Baseline Characteristics

Baseline characteristics of the study subjects are summarized in Table 1. Twenty-two subjects were assigned to group A (Fig. 1A), 12 to group B (Fig. 1B), and 77 to group C (Fig. 1C). Mean age of group A (27 ± 22) was significant younger than those in group B (40 ± 24) and group C (50 ± 17). There were no differences in prevalence of the gene mutations between the three groups. Maximal wall thickness and interventricular septal wall thickness of group C (18.9 ± 4.5 mm and 17.9 ± 4.7) were significantly greater than those in groups A (9.1 ± 1.8 and 8.7 ± 1.9) and B (10.3 ± 1.9 and 9.8 ± 2.1). There were no differences in maximal wall thickness and interventricular septal wall thickness between groups A and B. Left ventricular dimensions and left ventricular fractional shortening were not different among the three groups.

### QT Variables in the Study Groups

QT variables in the study groups are summarized in Table 2. Maximum QTc interval and QT